arXiv:1309.7376v1 [math.ST] 27 Sep 2013

A NEW TEST FOR ONE-WAY ANOVA WITH FUNCTIONAL DATA AND APPLICATION TO ISCHEMIC HEART SCREENING

JIN-TING ZHANG[⋆], MING-YEN CHENG[†], CHI-JEN TSENG[‡], AND HAU-TIENG WU[◊]

ABSTRACT. We propose and study a new global test, namely the $F_{\max}$-test, for the one-way ANOVA problem in functional data analysis. The test statistic is taken as the maximum value of the usual pointwise F-test statistics over the interval the functional responses are observed. A nonparametric bootstrap method is employed to approximate the null distribution of the test statistic and to obtain an estimated critical value for the test. The asymptotic random expression of the test statistic is derived and the asymptotic power is studied. In particular, under mild conditions, the $F_{\max}$-test asymptotically has the correct level and is root-n consistent in detecting local alternatives. Via some simulation studies, it is found that in terms of both level accuracy and power, the $F_{\max}$-test outperforms the Globalized Pointwise F (GPF) test of Zhang & Liang (2013) when the functional data are highly or moderately correlated, and its performance is comparable with the latter otherwise. An application to an ischemic heart real dataset suggests that, after proper manipulation, resting electrocardiogram (ECG) signals can be used as an effective tool in clinical ischemic heart screening, without the need of further stress tests as in the current standard procedure.

keywords F-type test; L^2-norm based test; local power; myocardial ischemia; nonparametric bootstrap, pointwise F-test.

1. INTRODUCTION

Functional data are getting increasingly common in a wide scope of scientific fields ranging from climatology to medicine, from seismology to chemometrics, and so on. In addition, as data collection technology evolves, nowadays we can conveniently collect and record a huge amount of functional data. Compared with traditional data which consist of point observations, functional data might contain more detailed information about the underlying system. On the other hand, new challenges arise in the endeavor to extract any meaningful information hidden in the often massive functional data at hand. In the past two decades, functional data analysis has emerged as an important area and significant progress has been achieved (Ramsay & Silverman, 2005; Ferraty, 2011; Zhang, 2013). In this paper we concentrate on the one-way ANOVA problem with functional responses, which is a fundamental problem in the inference but has received much less attention in functional data analysis compared to other problems such as regression. Besides, functional one-way ANOVA testing is closely related to classification, clustering and image analysis (Xue & Titterington, 2011; Slaets et al., 2012; Samworth, 2012; Hall et al., 2013).

A particular medical example is about ischemic heart which is treated in greater detail in Section 5: we ask if we can distinguish the group of normal subjects from the group of subjects with ischemic heart by reading their resting electrocardiogram (ECG) signals, which are clearly functional data. Traditional, based on the physiological facts, physicians "reduce the dimension" of an ECG signal by focusing on a specific subinterval, and then distinguish between the two groups based on this reduced information. Intuitively, we lose information about the system by doing so, and a direct consequence is that we are not able to distinguish between the group of normal subjects from the group of stable ischemic heart with the reduced data. Thus, in clinics, further stress tests are needed to assist the diagnosis. However, stress tests cannot be applied to patients who are vulnerable to acute attacks during the testing, which is associated with the stress itself. An immediate question we may ask is whether we can avoid the stress. In particular, we ask if there is a better way to differentiate between the normal and ischemic heart

[⋆] Department of Statistics and Applied Probability, National University of Singapore, Singapore.
[†] Department of Mathematics, National Taiwan University, Taiwan.
[‡] Cardiovascular Research Institute, Fooyin University Hospital, Taiwan.
[◊] Department of Mathematics, Stanford University, USA.

groups if we process the resting ECG signals properly during the diagnosis. In other words, we like to test equality of the mean functions of the two groups of manipulated ECG functions, and this is a special case of the one-way ANOVA hypothesis testing problem for functional data.

Let $y_{i1}(t), y_{i2}(t), \cdots, y_{in_i}(t)$, where $i = 1, 2, \cdots, k$, denote k groups of random functions defined over a given finite interval $\mathcal{T} = [a, b]$ and $n_i \in \mathbb{N}$ is the number of cases in the i-th group. Let SP(μ, γ) denote a stochastic process with mean function $\mu(t), t \in \mathcal{T}$, and covariance function $\gamma(s, t), s, t \in \mathcal{T}$. Assuming that

$$y_{i1}, y_{i2}, \cdots, y_{in_i} \overset{i.i.d.}{\sim} \text{SP}(\mu_i, \gamma),\ i = 1, 2, \cdots, k, \tag{1}$$

it is often interesting to test the equality of the k mean functions:

$$H_0 : \mu_1(t) = \mu_2(t) = \cdots = \mu_k(t),\ \forall t \in \mathcal{T}, \tag{2}$$

against the usual alternative that at least two of the mean functions are not equal. The above problem is known as the k-sample testing problem or the one-way ANOVA problem for functional data. For the above one-way ANOVA problem, the k mean functions are often decomposed as $\mu_i(t) = \mu_0(t) + \alpha_i(t), i = 1, 2, \cdots, k$, where $\mu_0(t)$ is the grand mean function and $\alpha_i(t), i = 1, 2, \cdots, k$, are the k main-effect functions so that the null hypothesis (2) is often equivalently written as the problem of testing if the main-effect functions are all zero, i.e., $H_0 : \alpha_1(t) = \alpha_2(t) = \cdots = \alpha_k(t) = 0, \forall t \in \mathcal{T}$.

There are several existing methods for testing the one-way ANOVA problem (2). The L^2-norm based test and the F-type test for linear models with functional responses (Faraway, 1997; Shen & Faraway, 2004; Zhang & Chen, 2007; Zhang, 2011) may be adopted for this purpose; see Zhang & Liang (2013) for more details. Cuevas et al. (2004) proposed and studied an L^2-norm based test directly for testing (2). They derived the limit random expression of their test statistic and suggested to approximate the null distribution by a parametric bootstrap method via re-sampling from the Gaussian process involved in the limit random expression under the null hypothesis. In addition, the pointwise F-test was proposed by Ramsay & Silverman (2005), naturally extending the classical F-test to the context of functional data analysis; see also Zhang (2013). It's test statistic is defined as

$$F_n(t) = \frac{\text{SSR}_n(t)/(k-1)}{\text{SSE}_n(t)/(n-k)}, \tag{3}$$

where and throughout, $n = \sum_{i=1}^k n_i$ denotes the total sample size,

$$\text{SSR}_n(t) = \sum_{i=1}^k n_i[\bar{y}_{i.}(t) - \bar{y}_{..}(t)]^2 \ \text{ and } \ \text{SSE}_n(t) = \sum_{i=1}^k \sum_{j=1}^{n_i} [y_{ij}(t) - \bar{y}_{i.}(t)]^2 \tag{4}$$

denote the pointwise between-subject and within-subject variations respectively, and

$$\bar{y}_{..}(t) = \frac{1}{n} \sum_{i=1}^k \sum_{j=1}^{n_i} y_{ij}(t) \ \text{ and } \ \bar{y}_{i.}(t) = \frac{1}{n_i} \sum_{j=1}^{n_i} y_{ij}(t),\ i = 1, \ldots, k, \tag{5}$$

are the sample grand mean function and the sample group mean functions respectively. Then, the null hypothesis (2) is rejected as long as the pointwise null hypothsis $H_{0t} : \mu_1(t) = \mu_2(t) = \cdots = \mu_k(t)$ is rejected at any point $t \in \mathcal{T}$.

There are a few advantages of using the above pointwise F-test. Denote by $F_{p,q}$ the F-distribution with p and q degrees of freedom. When the functional data (1) are realizations of Gaussian processes, under the null hypothesis (2) $F_n(t)$ follows the $F_{k-1,n-k}$ distribution for any given $t \in \mathcal{T}$. Therefore, for any pre-determined significance level α, we can test the null hypothesis (2) at all of the points in $\mathcal{T}$ using the same critical value $F_{k-1,n-k}(\alpha)$ where $F_{k-1,n-k}(\alpha)$ denotes the upper 100α percentile of the $F_{k-1,n-1}$ distribution. On the other hand, the pointwise F-test has some limitations too. For example, for a given significance level, it is not guaranteed that alternative hypothesis in the one-way ANOVA problem is overall significant even when the pointwise F-test is significant for each point in $\mathcal{T}$ at the same significance level. To overcome this difficulty, Cox & Lee (2008) proposed to correct the pointwise P-values of the pointwise F-tests via incorporating some Bonferroni-type multiple comparison idea. The

resulting pointwise F-test, however, becomes very complicated since the corrected pointwise P-values are obtained via intensive bootstrapping. Therefore, some simple method for summarizing the pointwise F-tests is desirable. To this end, Zhang & Liang (2013) proposed and studied a so-called Globalized Pointwise F-test, abbreviated as GPF test, whose test statistic is taken as the integral of the pointwise F-test statistic over $\mathcal{T}$:

$$T_n = \int_{\mathcal{T}} F_n(t)dt. \tag{6}$$

Via some simulation studies, Zhang & Liang (2013) showed that in terms of size-controlling and power, the GPF test is in general comparable with the L^2-norm based test and the F-type test adopted for the one-way ANOVA problem (2).

Alternatively, as pointed out by Zhang & Liang (2013), one can also globalize the pointwise F-test using the supremum of the pointwise F test statistic over $\mathcal{T}$:

$$F_{\max} = \sup_{t\in\mathcal{T}} F_n(t). \tag{7}$$

This $F_{\max}$-test is somewhat similar to the one suggested in Ramsay & Silverman (2005) (p.234) where they used the squared-root of $F_n(t)$ as their test statistic and used a permutation-based critical value. In Zhang & Liang (2013), the critical value of the $F_{\max}$-test was obtained via bootstrapping. By an application of the $F_{\max}$-test to a real functional dataset, Zhang & Liang (2013) realized that the $F_{\max}$-test may have higher power than their GPF test, particularly when the functional data are highly or moderately correlated. In addition, when applied to an ischemic heart ECG dataset, the $F_{\max}$-test was significant while the GPF test was not, which lead to contradictory answers to the relevant question arising from clinical ischemic heart screening. Therefore, a further study on the asymptotical and finite sample behaviors, in particular in terms of level accuracy and power, of the $F_{\max}$-test is necessary.

The major contributions of this paper are as follows. First of all, we derive the asymptotic random expression of the $F_{\max}$ test statistic under very general conditions and the null hypothesis (2). This allows us to prescribe a parametric bootstrap (PB) method for approximating the asymptotic null distribution of the $F_{\max}$ test statistic. However, one difficulty of this PB method is that it relies on the asymptotic random expression, which means that it is applicable only when the sample sizes $n_1, \ldots, n_k$ are all large. To overcome this difficulty, we propose a nonparametric bootstrap (NPB) method to approximate the null distribution of $F_{\max}$. Via some extensive simulation studies, we found that the simulated null probability density function (pdf) of the $F_{\max}$ test statistic is skewed when the functional data are moderately or highly correlated, and the estimated null pdf of the $F_{\max}$ test statistic using the NPB method approximates it reasonably well. Secondly, we show that the NPB $F_{\max}$-test has the correct asymptotic level, and it is root-n consistent i.e. its power tends to 1 under local alternatives that depart from the null hypothesis at the order $n^{-1/2}$. Thirdly, via some simulation studies, we show that in general the $F_{\max}$-test outperforms the GPF test of Zhang & Liang (2013) in terms of size-controlling, and the $F_{\max}$-test is substantially more powerful than the GPF test when the functional data are highly or moderately correlated while the former slightly performs worse than the latter otherwise. This latter result is intuitively reasonable: when the functional data are highly correlated the GPF test tends to average down the information provided by the data and hence has lower power than the $F_{\max}$-test, whereas when the functional data are less correlated the GPF test tends to summarize more uncorrelated information than the $F_{\max}$-test since the latter takes into account only the information at the maximum of the process $F_n(t)$. Since functional data are usually highly or moderately correlated, the $F_{\max}$-test is therefore preferred to the GPF test in general. This effect also explains the aforementioned contradictory results given by the $F_{\max}$ and GPF tests in the ischemic heart example: the ECG signals are highly correlated and only the $F_{\max}$-test (not the GPF test) detects the significant difference between the ECG signals of the normal and those of stable ischemic heart groups. Thus the $F_{\max}$-test result does suggest that it may be feasible to use solely ECG signals in ischemic heart screening, without the aid of more risky stress tests which is required in the current clinical practice. Lastly, we mention that it is straightforward to extend the $F_{\max}$-test to other linear regression models for functional data, including higher-way ANOVA for functional data and functional linear models with functional responses.

The rest of this paper is organized as follows. The main theoretical results on the level accuracy and local power of the $F_{\max}$-test are presented in Section 2. In Section 3 we study the discretization effect on the $F_{\max}$-test, and show that under mild conditions the discretization effect is negligible in terms of both size-controlling and local power. Results of extensive simulation studies and the real data example on ischemic heart screening based on ECG signals are given in Sections 4 and 5 respectively. Some concluding remarks are given in Section 6. Proofs of the theorectical results are deferred to the Appendix.

2. Main Results

2.1. **Asymptotic Random Expression under the Null Hypothesis.** We first derive the asymptotic random expression of the $F_{\max}$-test under the null hypothesis (2). This study will be helpful for approximating the null distribution of the $F_{\max}$-test. Notice that for any $t \in \mathcal{T}$, the pointwise between-subject variation $\text{SSR}_n(t)$ given in (4) can be expressed as

$$\text{SSR}_n(t) = [\mathbf{z}_n(t) + \boldsymbol{\mu}_n(t)]^T (\mathbf{I}_k - \mathbf{b}_n\mathbf{b}_n^T/n) [\mathbf{z}_n(t) + \boldsymbol{\mu}_n(t)], \tag{8}$$

where $\mathbf{I}_k$ is the $k \times k$ identity matrix,

$$\begin{aligned} \mathbf{z}_n(t) &= \left[\sqrt{n_1}[\bar{y}_{1.}(t) - \mu_1(t)], \sqrt{n_2}[\bar{y}_{2.}(t) - \mu_2(t)], \cdots, \sqrt{n_k}[\bar{y}_{k.}(t) - \mu_k(t)]\right]^T, \\ \boldsymbol{\mu}_n(t) &= [\sqrt{n_1}\mu_1(t), \sqrt{n_2}\mu_2(t), \cdots, \sqrt{n_k}\mu_k(t)]^T, \\ \mathbf{b}_n &= [\sqrt{n_1}, \sqrt{n_2}, \cdots, \sqrt{n_k}]^T. \end{aligned} \tag{9}$$

Since $\mathbf{b}_n^T\mathbf{b}_n/n = 1$, it is easy to verify that $\mathbf{I}_k - \mathbf{b}_n\mathbf{b}_n^T/n$ is an idempotent matrix with rank $k-1$. In addition, as $n \to \infty$, we have

$$\mathbf{I}_k - \mathbf{b}_n\mathbf{b}_n^T/n \to \mathbf{I}_k - \mathbf{b}\mathbf{b}^T, \text{ with } \mathbf{b} = [\sqrt{\tau_1}, \sqrt{\tau_2}, \cdots, \sqrt{\tau_k}]^T, \tag{10}$$

where $\tau_i = \lim_{n\to\infty} n_i/n,\ i = 1, 2, \cdots, k$, are as given in Condition A3 below. Note that $\mathbf{I}_k - \mathbf{b}\mathbf{b}^T$ in (10) is also an idempotent matrix of rank $k-1$, which has the following singular value decomposition:

$$\mathbf{I}_k - \mathbf{b}\mathbf{b}^T = \mathbf{U}\begin{pmatrix} \mathbf{I}_{k-1} & \mathbf{0} \\ \mathbf{0}^T & 0 \end{pmatrix}\mathbf{U}^T, \tag{11}$$

where the columns of $\mathbf{U}$ are the eigenvectors of $\mathbf{I}_k - \mathbf{b}\mathbf{b}^T$. This property will be used in the derivation of the main results of this paper. Based on the k samples (1), the pooled sample covariance function is given by

$$\hat{\gamma}(s,t) = (n-k)^{-1}\sum_{i=1}^{k}\sum_{j=1}^{n_i}[y_{ij}(s) - \bar{y}_{i.}(s)][y_{ij}(t) - \bar{y}_{i.}(t)], \tag{12}$$

where $\bar{y}_{i.}(t), i = 1, 2, \cdots, k$ are the sample group mean functions given in (5).

Let $\mathcal{L}^2(\mathcal{T})$ denote the set of all square-integrable functions over $\mathcal{T}$ and let $C^\beta(\mathcal{T})$, where $0 < \beta \le 1$, denote the set of functions f over $\mathcal{T}$ which are Hölder continuous with exponent β and Hölder modulus $\|f\|_{C^\beta}$. Let $\text{tr}(\gamma) = \int_{\mathcal{T}} \gamma(t,t)dt$ denote the trace of the covariance function $\gamma(s,t)$. For the theorectical study, we list the following regularity conditions.

Condition A

(1) The k population mean functions $\mu_1(t), \mu_2(t), \cdots, \mu_k(t)$ in (1) all belong to $\mathcal{L}^2(\mathcal{T})$.
(2) The subject-effect functions $v_{ij}(t) = y_{ij}(t) - \mu_i(t), j = 1, 2, \cdots, n_i; i = 1, 2, \cdots, k$, are i.i.d. $\text{SP}(0, \gamma)$ where 0 denotes the zero function whenever there is no ambiguity.
(3) As $n \to \infty$, the k sample sizes $n_1, \ldots, n_k$ satisfy $n_i/n \to \tau_i,\ i = 1, 2, \cdots, k$, such that $\tau_1, \tau_2, \cdots, \tau_k \in (0, 1)$.
(4) The subject-effect function $v_{11}(t)$ satisfies $\text{E}\|v_{11}\|^4 = \text{E}\left[\int_{\mathcal{T}} v_{11}^2(t)dt\right]^2 < \infty$.
(5) The covariance function $\gamma(s,t)$ satisfies $\gamma \in C^{2\beta}(\mathcal{T} \times \mathcal{T})$ with $\text{tr}(\gamma) < \infty$, where $0 < 2\beta \le 1$. For any $t \in \mathcal{T}$, $\gamma(t,t) > 0$.

(6) The expectation $\mathrm{E}\left[v_{11}^2(s)v_{11}^2(t)\right]$ is uniformly bounded. That is, for any $(s,t) \in \mathcal{T}\times\mathcal{T}$, we have $\mathrm{E}\left[v_{11}^2(s)v_{11}^2(t)\right] < C < \infty$ where C is some constant independent of (s,t).

The first two assumptions A1 and A2 are regular. Note $\mathcal{L}^2(\mathcal{T})$ functions may not be smooth. Condition A3 requires that the k sample sizes $n_1, n_2, \cdots, n_k$ tend to ∞ proportionally. This guarantees that as the total sample size $n \to \infty$, the sample group mean functions $\bar{y}_{i\cdot}(t), i = 1, 2, \cdots, k$, will converge to some Gaussian processes weakly. The last three assumptions A4, A5 and A6 are imposed so that the pointwise F-statistic $F_n(t)$ is well defined at any $t \in \mathcal{T}$ and the pooled sample covariance function $\hat{\gamma}(s,t)$ given in (12) converges to the population covariance function $\gamma(s,t)$ uniformly over $\mathcal{T}\times\mathcal{T}$.

Let $\mathrm{GP}_k(\boldsymbol{\mu}, \boldsymbol{\Gamma})$ denote "a k-dimensional Gaussian process with vector of mean functions $\boldsymbol{\mu}(t), t \in \mathcal{T}$, and matrix of covariance functions $\boldsymbol{\Gamma}(s,t), s,t \in \mathcal{T}$". We write $\boldsymbol{\Gamma}(s,t) = \gamma(s,t)\mathbf{I}_k$ for simplicity when $\boldsymbol{\Gamma}(s,t) = \mathrm{diag}\left[\gamma(s,t), \gamma(s,t), \cdots, \gamma(s,t)\right]$. In particular, $\mathrm{GP}(\eta, \gamma)$ denotes "a Gaussian process with mean function $\eta(t)$ and covariance function $\gamma(s,t)$". Further, let "$\xrightarrow{d}$" denote "converge in distribution" in the sense of (Laha & Rohatgi, 1979, p. 474) and (van der Vaart & Wellner, 1996, p. 50-51). Further, let "$X \overset{d}{=} Y$" denote that "X and Y have the same distribution." By Lemma A.1 in the Appendix, we can derive the asymptotical random expression of $F_{\max}$ under the null hypothesis (2) as given in the following proposition.

Proposition 2.1. Under Condition A and the null hypothesis (2), as $n \to \infty$, we have $F_{\max} \xrightarrow{d} R_0$ with

$$R_0 \overset{d}{=} \sup_{t\in\mathcal{T}} \left\{(k-1)^{-1}\sum_{i=1}^{k-1} w_i^2(t)\right\}, \tag{13}$$

where $w_1, w_2, \cdots, w_{k-1} \overset{i.i.d.}{\sim} \mathrm{GP}(0, \gamma_w)$ with $\gamma_w(s,t) = \gamma(s,t)/\sqrt{\gamma(s,s)\gamma(t,t)}$.

Proposition 2.1 is useful in discussing a PB method and in investigating an NPB method, detailed in next subsection, for approximating the null distribution of the $F_{\max}$ test statistic.

2.2. **Approximating the Null Distribution.** By Proposition 2.1, $w_1, \cdots, w_{k-1} \overset{i.i.d.}{\sim} \mathrm{GP}(0, \gamma_w)$ which is known except for $\gamma_w(s,t)$. The covariance function $\gamma_w(s,t)$ can be estimated as

$$\hat{\gamma}_w(s,t) = \frac{\hat{\gamma}(s,t)}{\sqrt{\hat{\gamma}(s,s)\hat{\gamma}(t,t)}}, \tag{14}$$

where $\hat{\gamma}(s,t)$ is the pooled sample covariance function given in (12). In this case, we can adopt the PB method in Cuevas et al. (2004) to construct an $F_{\max}$-test. The key idea is, for any given significance level α, to approximate the critical value of the $F_{\max}$-test statistic using the associated upper 100α-percentile of the random variable R_0. Here, based on (13), we can sample the i.i.d. Gaussian processes $w_i, i = 1, 2, \cdots, k-1$, from $\mathrm{GP}(0, \hat{\gamma}_w)$ a large number of times so that a large sample of R_0 can be obtained and hence the desired upper 100α-percentile of R_0 can be computed accordingly. It is obvious that this PB method approximates the critical values well only for large sample sizes.

To overcome the above difficulty of the PB method, we propose an NPB method for approximating the null distribution of the $F_{\max}$ test statistic which is applicable for both large and finite sample sizes. Denote the estimated subject-effect functions as

$$\hat{v}_{ij}(t) = y_{ij}(t) - \bar{y}_{i\cdot}(t),\ j = 1, 2, \cdots, n_i; i = 1, 2, \cdots, k, \tag{15}$$

which can be regarded as estimators of the subject-effect functions $v_{ij}(t), j = 1, 2, \cdots, n_{ij}, i = 1, 2, \cdots, k$, defined in Condition A2. Let

$$v_{ij}^*(t), j = 1, 2, \cdots, n_i; i = 1, 2, \cdots, k, \tag{16}$$

be bootstrapped k samples randomly generated from the estimated subject-effect functions given in (15). The nonparametric bootstrapped $F_{\max}$ test statistic can then be obtained as

$$F_{\max}^* = \sup_{t\in\mathcal{T}} F_n^*(t), \quad \text{where } F_n^*(t) = \frac{\mathrm{SSR}_n^*(t)/(k-1)}{\mathrm{SSE}_n^*(t)/(n-k)}, \tag{17}$$

with $\text{SSR}_n^*(t)$ and $\text{SSE}_n^*(t)$ obtained from (4) but based on the bootstrapped k samples (16). Repeat the above bootstrapping process a large number of times and calculate the upper 100α-percentile of the bootstrap sample on $F_{\max}^*$, and then conduct the level-α $F_{\max}$-test using this as the critical value.

Let C_α and C_α^* denote the upper 100α-percentiles of R_0 and $F_{\max}^*$ respectively, where R_0 is the limit random variable of $F_{\max}$ under the null hypothesis H_0 as defined in Proposition 2.1. The following proposition shows that the bootstrapped $F_{\max}$-test statistic $F_{\max}^*$ admits the same limit random expression R_0 and hence C_α^* will also tend to C_α in distribution as $n \to \infty$. Thus the $F_{\max}$-test based on the critical value C_α^* has the correct level α asymptotically.

Proposition 2.2. Under Condition A, as $n \to \infty$, we have $F_{\max}^* \xrightarrow{d} R_0$ and $C_\alpha^* \xrightarrow{d} C_\alpha$.

Notice that Proposition 2.2 holds under both the null and the alternative hypotheses. This is a desirable property since in practice either of the null and alternative hypotheses may be true. This property is mainly due to the fact that given the original k samples (1), the k bootstrapped samples (16) all have the same group mean function as 0 and hence the null hypothesis always holds for the bootstrapped k samples (16).

Proposition 2.2 shows that for large samples, the NPB method and the PB method will yield similar approximate critical values for the $F_{\max}$ test statistic. However, the PB method may involve more computational efforts since it requires sampling the Gaussian processes $w_i, i = 1, 2, \cdots, k-1$, from $\text{GP}(0, \hat{\gamma}_w)$ repeatedly. This may not be an easy task when calculation of $\hat{\gamma}(s,t)$ is challenging. Besides, larger samples sizes, which may not be available in some applications, are necessary for the PB method to work, in particular when the distribution of R_0 is skewed. In general, we prefer the NPB method to the PB method since it can be used under more general conditions than those required by the PB method and its implementation is relatively simple and efficient.

2.3. **The Asymptotic Power.** To study the asymptotic power of the proposed $F_{\max}$-test, we specify the following local alternative:

$$H_{1n}: \ \mu_i(t) = \mu_0(t) + n_i^{-1/2} d_i(t), \ i = 1, 2, \cdots, k, \tag{18}$$

where $\mu_0(t)$ is the grand mean function, and $d_1(t), \cdots, d_k(t)$ are any fixed real functions, independent of n. By (18), we have $\boldsymbol{\mu}(t) = [\mu_1(t), \cdots, \mu_k(t)]^T = \mu_0(t)\mathbf{1}_k + [n_1^{-1/2} d_1(t), \cdots, n_k^{-1/2} d_k(t)]^T$ where $\mathbf{1}_k$ denotes the $k \times 1$ vector of ones. It follows that $\boldsymbol{\mu}_n(t) = \mu_0(t)\mathbf{b}_n + \mathbf{d}(t)$ where $\boldsymbol{\mu}_n(t)$ is defined in (9) and $\mathbf{d}(t) = [d_1(t), \cdots, d_k(t)]^T$. Under Condition A3, as n tends to ∞, the local alternative (18) will tend to the null with the root-n rate. In this sense, if the $F_{\max}$-test can detect the local alternative (18) with probability 1 as long as the information provided by $\mathbf{d}(t)$ diverges to ∞, the $F_{\max}$- test is said to be root-n consistent. A good test usually should admit the root-n consistency. Notice that the local alternative (18) is the same as the one defined in Zhang & Liang (2013) who showed that their GPF test is root-n consistent. In this subsection, we shall show that the $F_{\max}$-test is also root-n consistent.

First, since $(\mathbf{I}_k - \mathbf{b}_n\mathbf{b}_n^T/n)\mathbf{b}_n = \mathbf{0}$, under the local alternative (18), we have

$$\text{SSR}_n(t) = \Big[\mathbf{z}_n(t) + \mathbf{d}(t)\Big]^T (\mathbf{I}_k - \mathbf{b}_n\mathbf{b}_n^T/n)\Big[\mathbf{z}_n(t) + \mathbf{d}(t)\Big], \tag{19}$$

where $\mathbf{z}_n(t)$ is defined in (9). We then have the following proposition about the asymptotic distribution of $F_{\max}$ under the local alternative (18).

Proposition 2.3. Under Condition A and the local alternative (18), as $n \to \infty$, we have $F_{\max} \xrightarrow{d} R_1$ with

$$R_1 \stackrel{d}{=} \sup_{t \in \mathcal{T}} \Big\{ (k-1)^{-1} \sum_{i=1}^{k-1} [w_i(t) + \delta_i(t)]^2 \Big\}, \tag{20}$$

where $w_1, \cdots, w_{k-1} \stackrel{i.i.d.}{\sim} \text{GP}(0, \gamma_w)$ as in Proposition 2.1 and $\delta_i(t), i = 1, 2, \cdots, k-1$, are the $k-1$ components of $\boldsymbol{\delta}(t) = (\mathbf{I}_{k-1}, \mathbf{0})\, \mathbf{U}^T \mathbf{d}(t)/\sqrt{\gamma(t,t)}$ with $\mathbf{U}$ given in (11).

With some abuse of notation, we set $\delta^2 = \sum_{i=1}^{k-1} \int_{\mathcal{T}} \delta_i^2(t)dt$, representing a summary of the information from $\mathbf{d}(t)$ with respect to the one-way ANOVA problem (2) where $\delta_i(t), i = 1, 2, \cdots, k-1$, are as defined in Proposition 2.3. By some simple calculations, we can write equivalently $\delta^2 = \int_{\mathcal{T}} \mathbf{h}(t)^T(\mathbf{I}_k - \mathbf{b}\mathbf{b}^T)\mathbf{h}(t)dt$ where $\mathbf{h}(t) = \mathbf{d}(t)/\sqrt{\gamma(t,t)}$. That is, this δ^2 is the same as the one defined and used in Propositions 2 and 3 in Zhang & Liang (2013). By using Proposition 3 in Zhang & Liang (2013), we can show the following proposition about the asymptotic power of the NPB $F_{\max}$-test.

Proposition 2.4. Under Condition A and the local alternative (18), as $n \to \infty$, the power of the NPB $F_{\max}$-test $P(F_{\max} \geq C_\alpha^*)$ tends to 1 as $\delta \to \infty$ where C_α^* is the upper 100α-percentile of the bootstrap test statistic $F_{\max}^*$ defined in (17).

Proposition 2.4 claims that the power of the $F_{\max}$-test under the local alternative (18) tends to 1 as the information provided by $\mathbf{d}(t)$ diverges, showing that the proposed $F_{\max}$-test is root n-consistent. In the proof of Proposition 2.4, we shall use the following relationship between the $F_{\max}$-test statistic defined in (7) and the GPF test statistic T_n defined in (6):

$$T_n = \int_{\mathcal{T}} F_n(t)dt \leq (b-a)F_{\max},$$

where we use the fact that $\mathcal{T} = [a, b]$. It then follows that

$$P(F_{\max} \geq C_\alpha^*) \geq P(T_n \geq (b-a)C_\alpha^*). \tag{21}$$

However, $(b-a)C_\alpha^*$ may not be equal or smaller than the upper (100α)-percentile of the GPF test statistic T_n. Thus, (21) does not guarantee that the $F_{\max}$-test has higher power than the GPF test. To compare the powers of the two tests, some simulation studies are then needed. Results of such simulation studies are summarized and discussed in Section 4.

3. Effect of Discretization on the $F_{\max}$ Test

We have studied the $F_{\max}$-test in the continuous setup in the previous sections. In practice, accessing the continuous functions $y_{ij}(t)\,, t \in \mathcal{T}$, $j = 1, \ldots, n_i$, $i = 1, \ldots, k$, may not be always possible, and in most scenarios we have only discretized observations on them. This issue has been partially discussed in Zhang & Chen (2007) by applying the local polynomial regression (LPR) scheme to reconstruct the continuous functions from the discretized samples and its asymptotical behavior has been studied therein. Specifically, when the function $\mu_i(t)$ is smooth enough and the discretization points follow some non-degenerate probability distribution function, LPR is applied to reconstruct $\mu_i(t)$. It is shown in Zhang & Chen (2007) that the LPR estimator is asymptotically unbiased and the convergence rate is discussed. However, in general $\mu_i(t)$ might not be that smooth, and the above approach cannot be applied. In this section we study a more direct approach to approximating the NPB $F_{\max}$-test under discretization and show that the approximation error incurred by discretization is negligible in terms of both the asymptotic level and the asymptotic power under local alternatives.

Suppose we observe the random functions $y_{ij}(t)$, $j = 1, \ldots, n_i$, $i = 1, \ldots, k$, in (1) only at some discretization points $t_1, \ldots, t_M$ of the interval $\mathcal{T} = [a, b]$, such that $t_1 = a$, $t_M = b$ and, for some positive $\tau_M = O(1/M)$ as $M \to \infty$,

$$0 < t_{l+1} - t_l \leq \tau_M, \text{ for all } l = 1, \ldots, M-1. \tag{22}$$

Note that the discretization might be non-uniform. Then we have k samples of random vectors; for $i = 1, \ldots, k$, the i-th sample consists of $\mathbf{y}_{ij,M} = (y_{ij}(t_1), \ldots, y_{ij}(t_M))^T$, $j = 1, \ldots, n_i$. Given the discretized samples $\{\mathbf{y}_{ij,M}\}_{j=1}^{n_i}$, $i = 1, \ldots, k$, we have access to the pointwise F test statistics at the discretization points: $F_n(t_l)$, $l = 1, \ldots, M$. Thus, parallel to the $F_{\max}$-test in the continuous-time case, we can test the discretized null hypothesis

$$H_{0,M} : \boldsymbol{\mu}_{1,M} = \ldots = \boldsymbol{\mu}_{k,M}. \tag{23}$$

using the following test statistic:

$$F_{\max,M} = \max_{l=1,\ldots,M} F_n(t_l). \tag{24}$$

For each $i = 1, \ldots, k$, based on the i-th discretized sample $\{\mathbf{y}_{ij,M}\}_{j=1}^{n_i}$, we can generate randomly bootstrapped sample $\{\mathbf{v}^*_{ij,M}\}_{j=1}^{n_i}$, from the estimated subject-effects vectors$\{\hat{\mathbf{v}}_{ij,M} = \mathbf{y}_{ij,M} - \bar{\mathbf{y}}_{i\cdot,M}\}_{j=1}^{n_i}$, which are the estimators of the discretized subject-effects vectors $\{\mathbf{v}_{ij,M} = \mathbf{y}_{ij,M} - \boldsymbol{\mu}_{i,M}\}_{j=1}^{n_i}$ where $\bar{\mathbf{y}}_{i\cdot,M} = n_i^{-1}\sum_{j=1}^{n_i}\mathbf{y}_{ij,M}$ and $\boldsymbol{\mu}_{i,M} = (\mu_i(t_1), \ldots, \mu_i(t_M))^T$ is the discretization of the mean function $\mu_i(t)$. The bootstrapped $F_{\max,M}$ test statistic is then obtained as

$$F^*_{\max,M} = \max_{l=1,\ldots,M} F^*_n(t_l), \tag{25}$$

where $F^*_n(t_l)$ are the bootstrap version of $F_n(t_l)$ based on the bootstrapped k samples $\{\mathbf{v}^*_{ij,M}\}_{j=1}^{n_i}$, $i = 1, 2, \cdots, k$. Repeat the above bootstrapping process a large number of times and calculate the upper 100α-percentile of $F^*_{\max,M}$. Then we can conduct accordingly the NPB $F_{\max,M}$-test for testing the discretized null hypothesis $H_{0,M}$ (23).

Let $N_l(\boldsymbol{\nu}, \boldsymbol{\Gamma})$ denote the distribution of an l-vector of Gaussian entries, which has mean vector $\boldsymbol{\nu}$ and covariance matrix $\boldsymbol{\Gamma}$. Proposition 3.1 studies the null distribution of $F_{\max,M}$.

Proposition 3.1. Suppose Condition A holds. Then, under the null hypothesis H_0 given in (2), we have $F_{\max,M} \xrightarrow{d} R_{0,M}$ as $n \to \infty$ where $R_{0,M} \stackrel{d}{=} \max_{l=1,\ldots,M}\left\{(k-1)^{-1}\sum_{i=1}^{k-1} w^2_{i,M}(l)\right\}$, with $\mathbf{w}_{i,M} \equiv (w_{i,M}(1), \ldots, w_{i,M}(M))^T, i = 1, \ldots, k-1, \stackrel{i.i.d.}{\sim} N_M(0, \boldsymbol{\Gamma}_{w,M})$ and $\boldsymbol{\Gamma}_{w,M} = \left(\gamma_w(t_p, t_q)\right)_{p,q=1,\ldots,M}$. In addition, for any given discretization $\{t_l\}_{l=1}^M$ of $\mathcal{T}$ satisfying (22), we may choose $\tilde{\beta}$ such that $0 < \tilde{\beta} < \beta$ and with probability tending to 1, we have $\left|R_0 - R_{0,M}\right| \le \tilde{c}\tau_M^{\tilde{\beta}}$, where R_0 is defined in (13) and the constant $\tilde{c}$ depends on the chosen $\tilde{\beta}$.

Let $C_{\alpha,M}$ and $C^*_{\alpha,M}$ denote the upper 100α-percentiles of $R_{0,M}$ and $F^*_{\max,M}$ respectively. Proposition 3.2 shows that the bootstrapped $F_{\max,M}$-test statistic $F^*_{\max,M}$ converges in distribution to the same $R_{0,M}$ as the $F_{\max,M}$-test statistic does under H_0, and hence $C^*_{\alpha,M}$ will also tend to $C_{\alpha,M}$ in distribution as $n \to \infty$. Thus, the $F_{\max,M}$-test based on the bootstrap critical value $C^*_{\alpha,M}$ has the correct asymptotic level for testing the discretized null hypothesis (23). In addition, the second result in Proposition 3.1 implies that $F_{\max,M}$ and $F_{\max}$ have the same limit test statistic R_0 under the null hypothesis, thus the NPB $F_{\max,M}$-test for testing (23) has the same asymptotic level as the NPB $F_{\max}$-test for testing H_0.

Proposition 3.2. Under Condition A, $F^*_{\max,M} \xrightarrow{d} R_{0,M}$ and $C^*_{\alpha,M} \to C_{\alpha,M}$ as $n \to \infty$.

Next, we study the local power of the NPB $F_{\max,M}$-test under the local alternative H_1 given in (18). The asymptotic distribution of the $F_{\max,M}$-test statistic under H_1 is given in the following proposition.

Proposition 3.3. Suppose Condition A holds. Then, under the local alternative H_1, as $n \to \infty$, we have $F_{\max,M} \xrightarrow{d} R_{1,M}$, where $R_{1,M} \stackrel{d}{=} \max_{l=1,\ldots,M}\left\{(k-1)^{-1}\sum_{i=1}^{k-1}[w_{i,M}(l) + \delta_{i,M}(l)]^2\right\} w_{i,M}(l), l = 1, \ldots, M$, are defined in Proposition 3.1 and $\delta_{i,M}(l), i = 1, 2, \cdots, k-1$, are the $k-1$ components of $\boldsymbol{\delta}_M(l) = (\mathbf{I}_{k-1}, \mathbf{0})\,\mathbf{U}^T\mathbf{d}(t_l)/\sqrt{\gamma(t_l, t_l)}$ with $\mathbf{U}$ given in (11). Furthermore, suppose $d_i \in C^{\tilde{\beta}}(\mathcal{T})$, $i = 1, \ldots, k$, for a given $0 < \tilde{\beta} < \beta$. Then, for any given discretization $\{t_l\}_{l=1}^M$ of $\mathcal{T}$ satisfying (22), with probability tending to 1, we have $\left|R_1 - R_{1,M}\right| \le \tilde{c}\tau_M^{\tilde{\beta}}$, where R_1 is defined in (20) and the constant $\tilde{c}$ depends on the chosen $\tilde{\beta}$ and the Hölder modulus of $d_i(t), i = 1, 2, \cdots, k$.

Combining the results in Propositions 3.1, 3.2 and 3.3, as $M \to \infty$, we have that the NPB $F_{\max,M}$-test has the same asymptotic power as the NPB $F_{\max}$-test under the local alternative H_1. Together with Proposition 2.4, this implies that under the local alternative H_1 the power of the NPB $F_{\max,M}$-test tends to 1, provided that $\mathbf{d}(t)$ diverges as $n \to \infty$ and both Condition A and (22) hold.

4. Simulation Studies

In this section, we present some results of simulation studies, aiming to check if the bootstrapped null distribution of the $F_{\max}$-test approximates the underlying null distribution of the $F_{\max}$-test well and how the $F_{\max}$-test is compared with the GPF test of Zhang & Liang (2013).

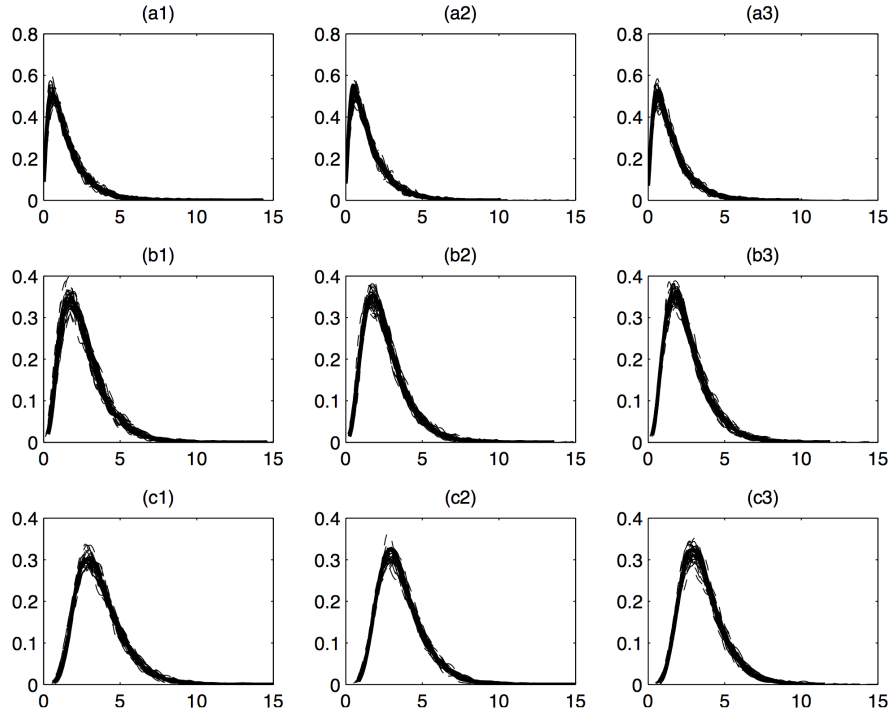

FIGURE 1. The simulated null pdfs (wider solid) and the first 50 bootstrapped null pdfs (dashed) of the $F_{\max}$-test when $z_{ijr}, r = 1, \cdots, q; j = 1, \cdots, n_i; i = 1, \cdots, k$, are i.i.d. $N(0,1)$ and $M = 80$. From left to right, the columns correspond to the sample size vectors $\mathbf{n}_1, \mathbf{n}_2$, and $\mathbf{n}_3$ respectively, and from top to bottom the rows correspond to $\rho = 0.10, 0.50$ and 0.90 respectively (those plots associated with $\rho = 0.30$ and 0.70 are not shown to save space).

The k functional samples (1) were generated from the following one-way ANOVA model:

$$\begin{aligned} y_{ij}(t) &= \mu_i(t) + v_{ij}(t), \;\; \mu_i(t) = \mathbf{c}_i^T[1, t, t^2, t^3]^T, \;\; v_{ij}(t) = \mathbf{b}_{ij}^T \mathbf{\Psi}(t), \; t \in [0,1], \\ \mathbf{b}_{ij} &= [b_{ij1}, b_{ij2}, \cdots, b_{ijq}]^T, \; b_{ijr} \stackrel{d}{=} \sqrt{\lambda_r} z_{ijr}, \; r = 1, 2, \cdots, q; \end{aligned} \tag{26}$$

$j = 1, 2, \cdots, n_i, i = 1, 2, \cdots, k$, where the parameter vectors $\mathbf{c}_i = [c_{i1}, c_{i2}, c_{i3}, c_{i4}]^T, i = 1, 2, \cdots, k$, for the group mean functions $\mu_i(t), i = 1, 2, \cdots, k$, can be flexibly specified, the random variables $z_{ijr}, r = 1, 2, \cdots, q; j = 1, 2, \cdots, n_i; i = 1, 2, \cdots, k$ are i.i.d. with mean 0 and variance 1, $\mathbf{\Psi}(t) = [\psi_1(t), \cdots, \psi_q(t)]^T$ is a vector of q orthonormal basis functions $\psi_r(t), t \in [0,1], r = 1, 2, \cdots, q$, and the variance components $\lambda_r, r = 1, 2, \cdots, q$ are positive and decreasing in r, and the number of the basis functions q is an odd positive integer. These tuning parameters help specify the group mean functions $\mu_i(t) = c_{i1} + c_{i2}t + c_{i3}t^2 + c_{i4}t^3, i = 1, 2, \cdots, k$ and the common covariance function $\gamma(s,t) = \mathbf{\Psi}(s)^T \text{diag}(\lambda_1, \lambda_2, \cdots, \lambda_q)\mathbf{\Psi}(t) = \sum_{r=1}^q \lambda_r \psi_r(s)\psi_r(t)$, of the subject-effect functions $v_{ij}(t), j = 1, 2, \cdots, n_i, i = 1, 2, \cdots, k$. In the simulations we considered, for simplicity, we assume that the design time points for all the functions $y_{ij}(t), j = 1, 2, \cdots, n_i, i = 1, 2, \cdots, k$ are the same and are specified as $t_j = j/(M+1), \; j = 1, \cdots, M$, where M is some positive integer. In practice, these functions can be observed at different design time points. In this case, some smoothing technique, such as the one discussed in Zhang & Liang (2013), can be used to reconstruct the functions $y_{ij}(t), j = 1, 2, \cdots, n_i, i = 1, 2, \cdots, k$, and then to evaluate them at a common grid of time points. This latter simulation setup will be time-consuming to carry out and we did not explore it in the simulations.

We now specify the model parameters in (26). To specify the group mean functions $\mu_1(t), \cdots, \mu_k(t)$, we set $\mathbf{c}_1 = [1, 2.3, 3.4, 1.5]^T$ and $\mathbf{c}_i = \mathbf{c}_1 + (i-1)\delta\mathbf{u}, i = 2, \cdots, k$, where the tuning parameter δ specifies the differences $\mu_i(t) - \mu_1(t), i = 2, \cdots, k$, and the constant vector $\mathbf{u}$ specifies the direction of these differences. We set δ properly as listed in Tables 1 and 2 below so that the null hypothesis (when

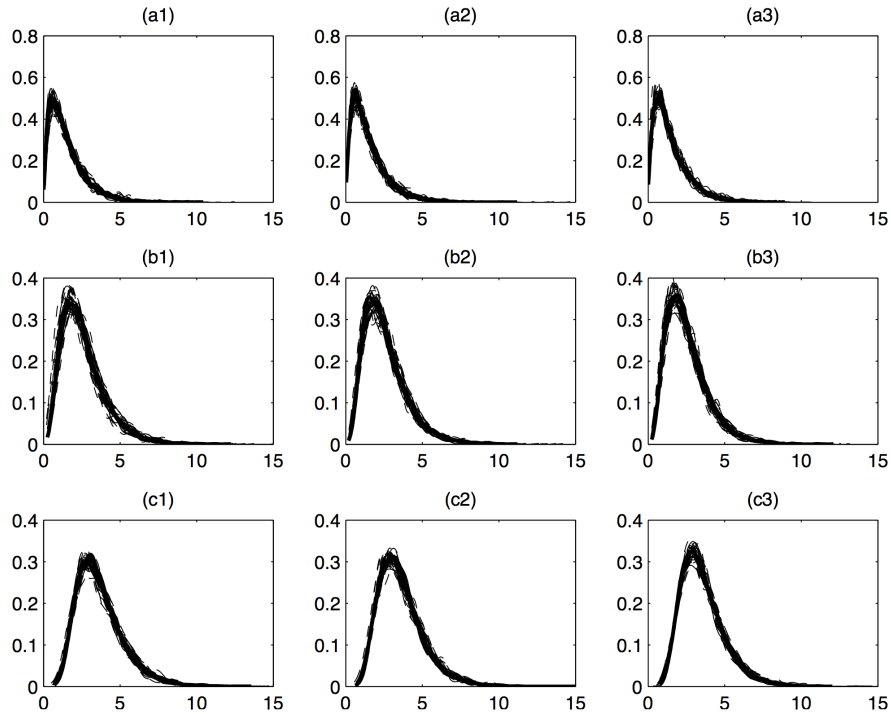

FIGURE 2. The same as in Fig. 1 except that now $z_{ijr}, r = 1, \cdots, q; j = 1, \cdots, n_i; i = 1, \cdots, k \overset{i.i.d.}{\sim} t_4/\sqrt{2}$.

$\delta = 0$) and the four alternatives (when $\delta > 0$) are fulfilled. In addition, we set $\mathbf{u} = [1, 2, 3, 4]^T/\sqrt{30}$ so that it is a unit vector. To specify the common covariance function $\gamma(s, t)$, for simplicity, we set $\lambda_r = a\rho^{r-1}, r = 1, 2, \cdots, q$, for some $a > 0$ and $0 < \rho < 1$. Notice that the tuning parameter ρ not only determines the decay rate of $\lambda_1, \cdots, \lambda_q$, but also determines how the simulated functional data are correlated: when ρ is close to 0, $\lambda_1, \cdots, \lambda_q$ will decay very fast, indicating that the simulated functional data are highly correlated; and when ρ is close to 1, $\lambda_r, r = 1, 2, \cdots, q$ will decay very slowly, indicating that the simulated functional data are nearly uncorrelated. For simplicity, we set the basis functions as $\psi_1(t) = 1$, $\psi_{2r}(t) = \sqrt{2}\sin(2\pi rt)$, $\psi_{2r+1}(t) = \sqrt{2}\cos(2\pi rt)$, $t \in [0, 1]$, $r = 1, \cdots, (q-1)/2$. In addition, we set $a = 1.5, q = 11$ and $\rho = 0.10, 0.30, 0.50, 0.70, 0.90$ to consider the five cases when the simulated functional data have very high, high, moderate, low, and very low correlations. We set the number of groups $k = 3$ and specified three cases of the sample size vector $\mathbf{n} = [n_1, n_2, n_3]$: $\mathbf{n}_1 = [20, 30, 30], \mathbf{n}_2 = [40, 30, 70]$ and $\mathbf{n}_3 = [80, 70, 100]$, representing the small, moderate and larger sample size cases respectively, and specify two cases of the number of design time points M: $M = 80$ and $M = 150$. Finally, we specified two cases of the distribution of the i.i.d. random variables $z_{ijr}, r = 1, \cdots, q;\ j = 1, \cdots, n_i;\ i = 1, \cdots, k$: $z_{ijr} \overset{i.i.d.}{\sim} N(0, 1)$ and $z_{ijr} \overset{i.i.d.}{\sim} t_4/\sqrt{2}$, allowing to generate Gaussian and non-Gaussian functional data respectively with z_{ijr} having mean 0 and variance 1. Notice that the $t_4/\sqrt{2}$ distribution is chosen since it has nearly the heaviest tails among the t-distributions with finite first two moments.

For a given model configuration, the k functional samples were generated as in (26) . Then the GPF test statistic and its P-value were computed. At the same time, the $F_{\max}$ test statistic was computed, and 10000 bootstrap replicates were generated to compute the P-value of the NPB $F_{\max}$-test. When the P-value of a testing procedure is smaller than the nominal significance level α (5% here), the null hypothesis (2) is rejected. The above process was repeated $N = 5000$ times. The empirical size or power of a testing procedure was then computed as the proportion of the number of rejections to the number of replications $N = 5000$.

TABLE 1. Empirical sizes and powers (in percentages) of the GPF and $F_{\max}$ tests for the functional one-way ANOVA problem (2) when the nominal level is 5%, $z_{ijr}, r = 1, \cdots, q; j = 1, \cdots, n_i; i = 1, \cdots, k$, are i.i.d. $N(0,1)$ and $M = 80$. The associated standard deviations (in percentages) are given in parentheses.

ρ	$\mathbf{n}$	GPF	$F_{\max}$	GPF	$F_{\max}$	GPF	$F_{\max}$	GPF	$F_{\max}$	GPF	$F_{\max}$	GPF	$F_{\max}$
		$\delta = 0$		$\delta = 0.03$		$\delta = 0.06$		$\delta = 0.10$		$\delta = 0.13$		$\delta = 0.16$	
0.10	$\mathbf{n}_1$	5.60	5.04	7.14	8.80	11.20	26.28	26.64	71.96	43.16	94.16	64.62	99.30
		(0.32)	(0.30)	(0.36)	(0.40)	(0.44)	(0.62)	(0.62)	(0.63)	(0.70)	(0.33)	(0.67)	(0.11)
	$\mathbf{n}_2$	5.54	5.09	8.68	16.03	20.82	58.60	54.66	98.06	81.64	100.00	96.02	100.00
		(0.32)	(0.31)	(0.39)	(0.51)	(0.57)	(0.69)	(0.70)	(0.19)	(0.54)	(0.00)	(0.27)	(0.00)
	$\mathbf{n}_3$	5.72	5.24	11.20	26.34	33.22	86.64	83.52	100.00	98.44	100.00	100.00	100.00
		(0.32)	(0.31)	(0.44)	(0.62)	(0.66)	(0.48)	(0.52)	(0.00)	(0.17)	(0.00)	(0.00)	(0.00)
		$\delta = 0$		$\delta = 0.05$		$\delta = 0.10$		$\delta = 0.15$		$\delta = 0.20$		$\delta = 0.25$	
0.30	$\mathbf{n}_1$	5.40	5.00	7.28	7.24	11.26	18.06	20.88	40.68	35.22	71.54	52.74	91.22
		(0.31)	(0.30)	(0.36)	(0.36)	(0.44)	(0.54)	(0.57)	(0.69)	(0.67)	(0.63)	(0.70)	(0.40)
	$\mathbf{n}_2$	5.84	5.02	8.98	11.10	20.22	39.60	41.30	81.49	70.56	98.70	89.94	100.00
		(0.33)	(0.30)	(0.40)	(0.44)	(0.56)	(0.69)	(0.69)	(0.54)	(0.64)	(0.16)	(0.42)	(0.00)
	$\mathbf{n}_3$	5.36	4.86	10.24	16.58	31.28	67.88	66.72	97.90	92.80	100.00	99.66	100.00
		(0.31)	(0.30)	(0.42)	(0.52)	(0.65)	(0.66)	(0.66)	(0.20)	(0.36)	(0.00)	(0.08)	(0.00)
		$\delta = 0$		$\delta = 0.10$		$\delta = 0.20$		$\delta = 0.30$		$\delta = 0.40$		$\delta = 0.50$	
0.50	$\mathbf{n}_1$	5.14	4.40	8.86	8.52	20.58	27.02	44.26	65.54	73.26	92.64	90.92	99.38
		(0.31)	(0.29)	(0.40)	(0.39)	(0.57)	(0.62)	(0.70)	(0.67)	(0.62)	(0.36)	(0.40)	(0.11)
	$\mathbf{n}_2$	4.84	4.40	13.03	15.93	42.82	64.38	80.02	97.24	98.34	99.98	99.96	100.00
		(0.30)	(0.29)	(0.47)	(0.51)	(0.69)	(0.67)	(0.56)	(0.23)	(0.18)	(0.01)	(0.02)	(0.00)
	$\mathbf{n}_3$	5.54	4.82	19.28	26.82	67.78	90.84	97.82	100.00	99.98	100.00	100.00	100.00
		(0.32)	(0.30)	(0.55)	(0.62)	(0.66)	(0.40)	(0.20)	(0.00)	(0.01)	(0.00)	(0.00)	(0.00)
		$\delta = 0$		$\delta = 0.20$		$\delta = 0.40$		$\delta = 0.60$		$\delta = 0.80$		$\delta = 1.00$	
0.70	$\mathbf{n}_1$	5.76	4.74	14.34	12.24	47.80	48.84	86.10	91.00	99.10	99.70	100.00	99.98
		(0.32)	(0.30)	(0.49)	(0.46)	(0.70)	(0.70)	(0.48)	(0.40)	(0.13)	(0.07)	(0.00)	(0.01)
	$\mathbf{n}_2$	4.86	4.63	25.84	26.16	83.86	89.36	99.82	100.00	100.00	100.00	100.00	100.00
		(0.30)	(0.29)	(0.61)	(0.62)	(0.52)	(0.43)	(0.05)	(0.00)	(0.00)	(0.00)	(0.00)	(0.00)
	$\mathbf{n}_3$	5.84	4.94	42.64	46.70	98.54	99.50	100.00	100.00	100.00	100.00	100.00	100.00
		(0.33)	(0.30)	(0.69)	(0.70)	(0.16)	(0.09)	(0.00)	(0.00)	(0.00)	(0.00)	(0.00)	(0.00)
		$\delta = 0$		$\delta = 0.30$		$\delta = 0.60$		$\delta = 0.90$		$\delta = 1.20$		$\delta = 1.50$	
0.90	$\mathbf{n}_1$	5.14	5.14	14.24	10.82	55.22	42.10	93.50	85.70	99.94	99.36	100.00	100.00
		(0.31)	(0.31)	(0.49)	(0.43)	(0.70)	(0.69)	(0.34)	(0.49)	(0.03)	(0.11)	(0.00)	(0.00)
	$\mathbf{n}_2$	5.12	5.09	29.82	23.02	92.12	84.62	99.96	99.94	100.00	100.00	100.00	100.00
		(0.31)	(0.31)	(0.64)	(0.59)	(0.38)	(0.51)	(0.02)	(0.03)	(0.00)	(0.00)	(0.00)	(0.00)
	$\mathbf{n}_3$	4.90	4.72	53.44	41.08	99.68	99.30	100.00	100.00	100.00	100.00	100.00	100.00
		(0.30)	(0.29)	(0.70)	(0.69)	(0.07)	(0.11)	(0.00)	(0.00)	(0.00)	(0.00)	(0.00)	(0.00)

$\mathbf{n}_1 = [20, 30, 30]$, $\mathbf{n}_2 = [40, 30, 70]$, $\mathbf{n}_3 = [80, 70, 100]$.

We first check if the bootstrapped null pdf of the $F_{\max}$ test statistic works well in approximating the underlying null pdf of the $F_{\max}$ test statistic. To this end, each panel in Fig. 1 displays the simulated null pdf (wider solid curve) and the first 50 bootstrapped null pdfs (dashed curves) of the $F_{\max}$ test statistic when $z_{ijr}, r = 1, \cdots, q; j = 1, \cdots, n_i; i = 1, \cdots, k \overset{i.i.d.}{\sim} N(0,1)$ and $M = 80$. Each of the pdfs was computed using the usual kernel density estimator (Wand & Jones, 1995, Ch. 2) based on the 5000 simulated $F_{\max}$ test statistics (7) or the 10000 bootstrapped $F_{\max}$ test statistic when $\delta = 0$ and $M = 80$. From Fig. 1, it is seen that the bootstrapped null pdfs of the $F_{\max}$ test statistic approximate the associated simulated null pdf rather well in all of the nine panels, showing that the NPB method does work reasonably well in approximating the underlying null pdfs of the $F_{\max}$ test statistic. Furthermore, it seems that the effects of the sample sizes are not remarkable; but the shapes of the simulated and bootstrapped null pdfs of the $F_{\max}$ test statistic are strongly affected by the decay rates of the variance components $\lambda_r, r = 1, 2, \cdots, q$, namely, stronger correlation in the functional data (ρ smaller) causes more skewness in the null distribution of $F_{\max}$.

In Fig. 2, we display the simulated and bootstrapped null pdfs of the $F_{\max}$-test when $z_{ijr}, r = 1, \cdots, q; j = 1, \cdots, n_i; i = 1, \cdots, k \overset{i.i.d.}{\sim} t_4/\sqrt{2}$. From Fig. 2, we can see that the NPB method still works reasonably well in approximating the underlying null pdf of the $F_{\max}$-test and that the shapes

TABLE 2. Empirical sizes and powers (in percentage) of the GPF and $F_{\max}$-tests for the functional one-way ANOVA problem (2) when the nominal size is 5%, $z_{ijr}, r = 1, \cdots, q; j = 1, \cdots, n_i; i = 1, \cdots, k$, are i.i.d. $t_4/\sqrt{2}$ and $M = 80$. The associated standard deviations (in percentage) are given in parentheses.

ρ	$\mathbf{n}$	GPF	$F_{\max}$	GPF	$F_{\max}$	GPF	$F_{\max}$	GPF	$F_{\max}$	GPF	$F_{\max}$	GPF	$F_{\max}$
		$\delta = 0$		$\delta = 0.03$		$\delta = 0.06$		$\delta = 0.10$		$\delta = 0.13$		$\delta = 0.16$	
0.10	$\mathbf{n}_1$	5.42	5.00	6.51	8.93	12.30	29.94	28.46	74.80	46.08	93.24	65.12	98.66
		(0.32)	(0.30)	(0.34)	(0.40)	(0.46)	(0.64)	(0.63)	(0.61)	(0.70)	(0.35)	(0.67)	(0.16)
	$\mathbf{n}_2$	5.26	4.80	8.00	15.24	21.92	62.02	55.92	97.34	82.56	99.86	95.64	99.98
		(0.31)	(0.30)	(0.38)	(0.50)	(0.58)	(0.68)	(0.70)	(0.22)	(0.53)	(0.05)	(0.28)	(0.01)
	$\mathbf{n}_3$	5.08	5.00	11.26	27.60	35.82	86.94	83.58	99.92	98.04	100.00	99.70	100.00
		(0.31)	(0.30)	(0.44)	(0.63)	(0.67)	(0.47)	(0.52)	(0.03)	(0.19)	(0.00)	(0.07)	(0.00)
		$\delta = 0$		$\delta = 0.05$		$\delta = 0.10$		$\delta = 0.15$		$\delta = 0.20$		$\delta = 0.25$	
0.30	$\mathbf{n}_1$	5.22	4.82	7.26	7.42	11.98	19.28	22.28	44.74	38.52	74.06	55.78	91.16
		(0.31)	(0.30)	(0.36)	(0.37)	(0.45)	(0.55)	(0.58)	(0.70)	(0.68)	(0.61)	(0.70)	(0.40)
	$\mathbf{n}_2$	5.14	4.72	7.98	11.04	20.98	42.60	43.58	81.66	70.42	97.72	89.78	99.74
		(0.31)	(0.29)	(0.38)	(0.44)	(0.57)	(0.69)	(0.70)	(0.54)	(0.64)	(0.21)	(0.42)	(0.07)
	$\mathbf{n}_3$	5.90	5.74	10.30	16.92	32.56	70.18	67.42	97.64	93.08	99.94	99.02	100.00
		(0.33)	(0.32)	(0.42)	(0.53)	(0.66)	(0.64)	(0.66)	(0.21)	(0.35)	(0.03)	(0.13)	(0.00)
		$\delta = 0$		$\delta = 0.10$		$\delta = 0.20$		$\delta = 0.30$		$\delta = 0.40$		$\delta = 0.50$	
0.50	$\mathbf{n}_1$	4.72	5.06	9.10	9.03	21.36	29.62	48.60	67.40	73.34	92.54	91.46	98.96
		(0.29)	(0.30)	(0.40)	(0.40)	(0.57)	(0.64)	(0.70)	(0.66)	(0.62)	(0.37)	(0.39)	(0.14)
	$\mathbf{n}_2$	4.97	4.78	13.80	17.08	44.24	65.58	80.64	96.36	97.58	99.84	99.72	99.98
		(0.30)	(0.30)	(0.48)	(0.53)	(0.70)	(0.67)	(0.55)	(0.26)	(0.21)	(0.05)	(0.07)	(0.01)
	$\mathbf{n}_3$	5.66	5.00	19.70	28.16	68.40	91.02	97.46	99.94	99.88	100.00	100.00	100.00
		(0.32)	(0.30)	(0.56)	(0.63)	(0.65)	(0.40)	(0.22)	(0.03)	(0.04)	(0.00)	(0.00)	(0.00)
		$\delta = 0$		$\delta = 0.20$		$\delta = 0.40$		$\delta = 0.60$		$\delta = 0.80$		$\delta = 1.00$	
0.70	$\mathbf{n}_1$	4.76	4.92	13.10	12.74	48.28	50.82	85.38	90.92	98.76	99.66	99.74	100.00
		(0.30)	(0.30)	(0.47)	(0.47)	(0.70)	(0.70)	(0.49)	(0.40)	(0.15)	(0.08)	(0.07)	(0.00)
	$\mathbf{n}_2$	4.86	4.48	27.26	26.42	84.76	89.74	99.50	99.92	99.98	100.00	99.98	100.00
		(0.30)	(0.29)	(0.62)	(0.62)	(0.50)	(0.42)	(0.09)	(0.03)	(0.01)	(0.00)	(0.01)	(0.00)
	$\mathbf{n}_3$	5.40	5.00	44.02	47.70	98.46	99.48	100.00	100.00	100.00	100.00	100.00	100.00
		(0.31)	(0.30)	(0.70)	(0.70)	(0.17)	(0.10)	(0.00)	(0.00)	(0.00)	(0.00)	(0.00)	(0.00)
		$\delta = 0$		$\delta = 0.30$		$\delta = 0.60$		$\delta = 0.90$		$\delta = 1.20$		$\delta = 1.50$	
0.90	$\mathbf{n}_1$	4.50	5.40	14.36	11.18	55.52	43.68	93.54	86.90	99.50	99.26	99.94	99.98
		(0.29)	(0.31)	(0.49)	(0.44)	(0.70)	(0.70)	(0.34)	(0.47)	(0.09)	(0.12)	(0.03)	(0.01)
	$\mathbf{n}_2$	4.76	5.08	29.92	23.16	91.68	85.52	99.92	100.00	100.00	100.00	100.00	100.00
		(0.30)	(0.31)	(0.64)	(0.59)	(0.39)	(0.49)	(0.03)	(0.00)	(0.00)	(0.00)	(0.00)	(0.00)
	$\mathbf{n}_3$	4.78	4.74	51.90	41.56	99.50	99.32	100.00	100.00	100.00	100.00	100.00	100.00
		(0.30)	(0.30)	(0.70)	(0.69)	(0.09)	(0.11)	(0.00)	(0.00)	(0.00)	(0.00)	(0.00)	(0.00)

$\mathbf{n}_1 = [20, 30, 30]$, $\mathbf{n}_2 = [40, 30, 70]$, $\mathbf{n}_3 = [80, 70, 100]$.

of the simulated and bootstrapped null pdfs of the $F_{\max}$-test are again strongly affected by the decay rates of the variance components $\lambda_r, r = 1, 2, \cdots, q$. We also observe that the effects of the sample sizes are comparably minor.

We now turn to check how the NPB $F_{\max}$-test is compared with the GPF test of Zhang & Liang (2013) for the one-way ANOVA problem (2) in terms of level accuracy and power. For this purpose, we summarize in Tables 1 and 2 the empirical sizes and powers (in percentages) of the GPF and $F_{\max}$-tests when $z_{ijr}, r = 1, \cdots, q; j = 1, \cdots, n_i; i = 1, \cdots, k$ are i.i.d. $N(0, 1)$ or $t_4/\sqrt{2}$, respectively. The associated standard deviations (in percentages) of these empirical sizes and powers are also given in the parentheses. From the columns associated with $\delta = 0$ in both tables, we see that in terms of size controlling, in general, the NPB $F_{\max}$-test outperforms the GPF test. From the columns associated with $\delta > 0$ in both tables, we also see that in terms of power, in general the NPB $F_{\max}$-test has higher powers than the GPF test except when the functional data are less correlated ($\rho = 0.90$) and the advantages of the NPB $F_{\max}$-test over the GPF test become more significant as the correlation in the functional data increases.

In the above, we only presented the simulation results when $M = 80$ since those when $M = 150$ are similar. From all these simulation studies, we conclude that the NPB method presented in this paper works reasonably well in approximating the underlying null pdf of the $F_{\max}$-test and in general the NPB

$F_{\max}$ test statistic outperforms the GPF test in terms of size-controlling and it generally has significantly higher powers than the GPF test when the functional data are moderately or strongly correlated.

5. Screening Myocardial Ischemia Using Resting Electrocardiac Signals

In this section we present an example where the NPB $F_{\max}$ is useful in discovering new methods in medical studies. Specifically, detecting myocardial ischemia (MI) is an important clinical mission, in particular in outpatient evaluations. Typical evaluations include resting surface electrocardiography (ECG) examination and non-invasive stress testing, for example, exercise ECG and the single-photon emission computed tomography (SPECT) thallium scan. Although resting ECG is a fundamental measure in this regard, compared with stress tests, it is not accurate enough in detecting MI in a typical chest pain clinic (Gibbons et al., 2003). On the other hand, while stress tests are more accurate than a resting ECG, they have limitations in clinics. Among the limitations, the most important one is the stress itself: it is associated with the risk of acute attacks during the testing. Thus, stress tests cannot be performed on patients who are extremely susceptible to the provocations used in the tests, and such patients have to directly undergo invasive tests (Gibbons et al., 2003).

Recent findings from biophysics and pathology interdisciplinary work (Swan, 1979), researches on the physical characteristics of myocardial strain in echocardiography (Urheim et al., 2000) and studies on electric signals (del Rio et al., 2005) have necessitated a reappraisal of the ECG information for detecting MI. For example, spectral analysis of the resting ECG signals from dogs revealed a shift from high- to low-frequency ranges in ischemia cases (Mor-Avi & Akselrod, 1990). Similar phenomena were associated with balloon inflations during percutaneous transcatheter angioplasty in MI patients (Abboud et al., 1987; Pettersson et al., 2000). Based on these findings, we hypothesize that the ischemic myocardium information is contained in the resting ECG signals with the proper manipulation, and the power spectrum of the manipulated ECG signal is shifted to the low frequency. To test this hypothesis, the following prospective clinical study was conducted and the proposed NPB $F_{\max}$ test was applied to assess the result.

5.1. **Study populations and categorization.** We designed this study to use the same procedures employed in daily clinical practice and enrolled 393 consecutive individuals who visited an outpatient clinic complaining of chest pain. We evaluated the possibility of myocardial ischemia based on published guidelines (Gibbons et al., 2002, 2003; Klocke et al., 2003). The institutional review board of the hospital approved this protocol. Patients completed all the examinations within a span of three months, and all provided written consent.

We studied the following two groups – an ischemic group and a normal group defined by the following procedure by taking the clinical procedures into account. The ischemic group consisted of patients who directly underwent a coronary arteriography (CAG) and diagnosed as MI and patients having positive exercise ECG and/or SPECT thallium scan. If a patient's exercise ECG was inconclusive, the result of SPECT thallium scan was used for classification. The normal group comprised of patients who had had at least one stress test, and any of the test results was negative. We excluded individuals based on any of the following criteria: (i) non-cardiac chest pain and a very low risk of developing MI; (ii) non-NSR (normal sinus rhythm); (iii) already underwent exercise ECG, but were non-diagnostic or intolerant of the SPECT thallium scan, and unwilling to undertake further evaluation; (iv) a heart rate of less than 40 beats per minute. In the end, 137 patients were eligible for the analysis – 71 patients in the ischemic group and 66 patients in the normal group. Please see Fig. 3 for the details.

5.2. **Data acquisition.** We acquired from each subject 85 seconds of 12-lead resting ECG signals of his/her first visit to the outpatient clinic. The signals were acquired at 500Hz and quantized at 12 bits across ± 10 mV (Bailey et al., 1990). The signals were passed through a digital low-pass filter with a -3dB cutoff at 60 Hz, and stored in double precision. Besides removing the inherent amplitude deviations, such as power line noise, thermal noise, etc., we preserved all possible physiological activities. The recorded 12 lead ECG signals for the i-th subject is denoted as a $12 \times \mathcal{N}$ matrix $\boldsymbol{e}^{(i)}$, $\mathcal{N} = 85 \times 500$,

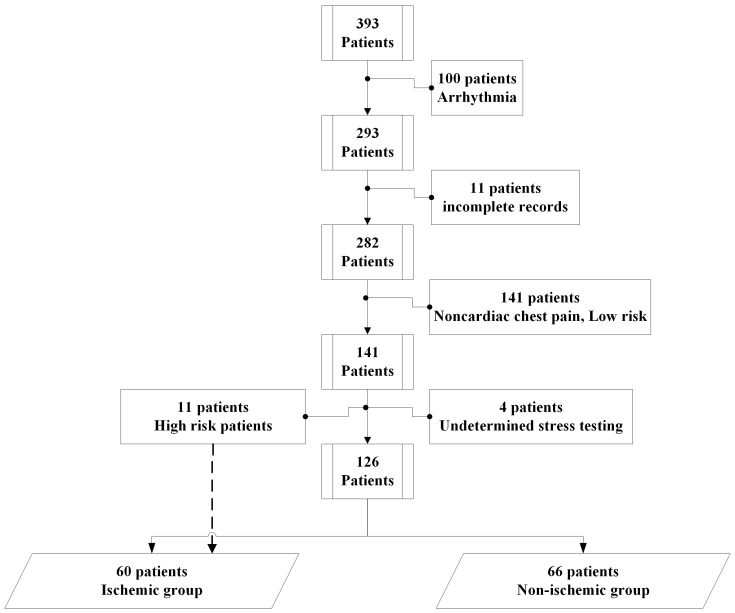

FIGURE 3. Flow chart of patient categories. Note that all 11 high-risk patients had had a positive CAG and remained in the ischemic group. In the end, there are 71 patients in the ischemic group and 66 patients in the normal group.

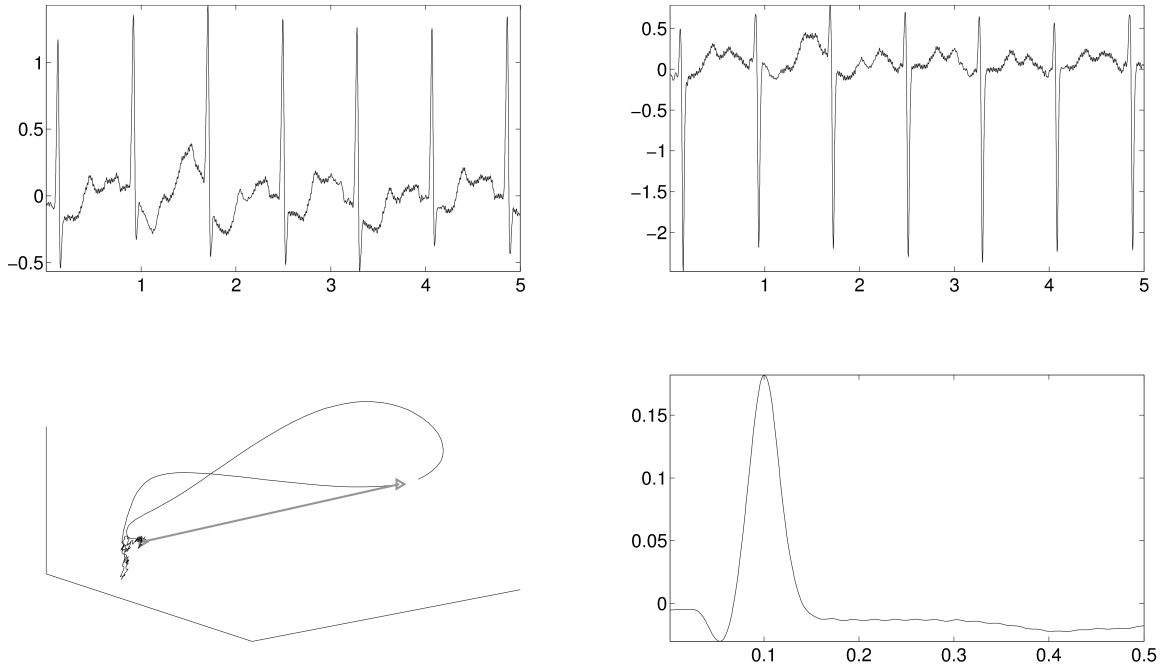

FIGURE 4. Upper left (right): a 5-second Lead II (Lead III) ECG signal. Lower left: the VCG signal of an extracted sinus heartbeat $\boldsymbol{b}^{(i,l)}$ (black curve) superimposed with the direction of $\mathbf{v}^{(i,l)}$ pointing from the origin (i.e. the atrio-ventricular node) to the R-peak (gray curve). Lower right: the adaptive lead signal $\mathbf{s}_0^{(i,l)}$ constructed by projecting $\boldsymbol{b}^{(i,l)}$ onto $\mathbf{v}^{(i,l)}$.

so that $\boldsymbol{e}^{(i)}(l,j)$ is the l-th lead ECG signal sampled at time $j\tau$, where $\tau = 1/500$ is the sampling interval and $j = 1, \ldots, \mathcal{N}$.

First, for the i-th subject, we reduced the influence of the lead system by recovering the 3-dimensional vectocardiograph (VCG) data with Levkovs algorithm (Levkov, 1987), which is denoted as a $3 \times \mathcal{N}$ matrix $V^{(i)}$, where the j-th column is the dipole current direction in $\mathbb{R}^3$ at time $j\tau$.

Second, we reduced the heart rate variability (HRV) effect. Denote $t^{(i,l)} \in \{1, \ldots, \mathcal{N}\}$ to be the indices of time stamps of the l-th R-peak of the n-th subject. The R-peaks were detected using the standard method (Clifford et al., 2006). We then extract the first L sinus heartbeat signals, where $L \in \mathbb{N}$. Here the l-th sinus heartbeat signal is the VCG signal between time $t^{(i,l)}\tau$ and $t^{(i,l+1)}\tau$. Denote the l-th extracted sinus heartbeat as a $3 \times (t^{(i,l+1)} - t^{(i,l)} + 1)$ matrix $\boldsymbol{b}_0^{(i,l)}$, where $\boldsymbol{b}_0^{(i,l)}(j, m) = \boldsymbol{e}^{(i)}(j, t^{(i,l)} + m - 1)$, $j = 1, \ldots, 3$ and $m = 1, \ldots, t^{(i,l+1)} - t^{(i,l)}$. Next, we interpolate each heartbeat by the cubic spline interpolation to be of the uniform length 500 to eliminate the HRV influence, and denote the l-th interpolated heartbeat as a 3×500 matrix $\boldsymbol{b}^{(i,l)}$. Then we "co-axial project" each interpolated heartbeat $\boldsymbol{b}^{(i,l)}$ onto the R-peak direction, which by our construction is the first column of $\boldsymbol{b}^{(i,l)}$. Denote this R-peak direction as a column vector $\mathbf{v}^{(i,l)} \in \mathbb{R}^3$, and we project $\boldsymbol{b}^{(i,l)}$ onto $\mathbf{v}^{(i,l)}$:

$$\mathbf{s}_0^{(i,l)} = [\mathbf{v}^{(i,l)}]^T \boldsymbol{b}^{(i,l)} \in \mathbb{R}^{1 \times N}.$$

We call $\mathbf{s}_0^{(i,l)}$ an *adaptive lead signal*, where the adjective *adaptive* means that the cardiac axis and lead system effects are reduced.

Third, we eliminated other physiological effects, in particular the respiration, by normalizing each beat $\mathbf{s}_0^{(i,l)}$ such that its L^2 norm is 1, which is denoted as another row vector $\mathbf{s}^{(i,l)}$ of length 500. With $\{\mathbf{s}^{(i,l)}\}_{l=1}^{L}$, the *adaptive ECG waveform* for the i-th subject is defined as

$$\mathbf{s}^{(i)} = \frac{1}{L} \sum_{l=1}^{L} \mathbf{s}^{(i,l)}. \tag{27}$$

We tested our null hypothesis based on the adaptive ECG waveform collected from the subjects. A typical ECG signal, the VCG signal and the adaptive ECG waveform representation are demonstrated in Fig. 4.

To confirm our hypothesis derived from the results in Mor-Avi & Akselrod (1990); Abboud et al. (1987); Pettersson et al. (2000), that is, the power spectrum of a beat of an ischemic heart is shifted to the low frequency region, we study the power spectrum of $\mathbf{s}^{(i)}$, which is defined as $P^{(i)} = |\mathcal{F}\mathbf{s}^{(i)}|^2$, where $\mathcal{F}$ is the discrete Fourier transform. Here $P^{(i)}$ is a row vector of length 500. We follow the convention and say the first entry of $P^{(i)}$ is the DC term, the second to 250 entries are of the positive frequencies and the left are of the negative frequencies. Further, we define the cumulative power spectrum of $\mathbf{s}^{(i)}$ as $f^{(i)}(m) = \sum_{j=2}^{m+1} P^{(i)}(j)$, where $m = 1, \ldots, 250$, that is $f^{(i)}$ is a row vector of length 250. Fig. 5 shows a set of adaptive ECG waveform $\mathbf{s}^{(i)}$ (upper row), power spectra $P^{(i)}$ (middle row) and the electrophysiological fingerprints $f^{(i)}$ (lower row).

5.3. $F_{\max}$ **Analysis and Results.** To test the one-way ANOVA problem (2) for the stable cardiac ischemia data, we considered the one-way ANOVA problem over the adaptive lead signal $\mathbf{s}_0^{(i,l)}$, the adaptive ECG waveform $\mathbf{s}^{(i)}$, its power spectrum $P^{(i)}$ and the cumulative power spectrum $f^{(i)}$. The associated P-values of the GPF and $F_{\max}$ tests are displayed in Table 3. It shows that the difference between the normal and ischemia groups was significant, at the 0.05 level, only when we applied the $F_{\max}$-test. The significance of the $F_{\max}$-test based on the adaptive ECG waveform indicates that the 12 lead ECG waveform does contain information about ischemic myocardium. However, this information is masked by the other physiological facts, like the lead system effect, the HRV and the respiration. HRV is the phenomenon of non-linear and non-stationary rhythms of heartbeats, caused by autonomic function, respiration and other physiological activities, even in resting conditions (Clifford et al., 2006). Thus, if we directly perform a Fourier transform to the 12 lead ECG signal, HRV would distort the result. In addition, lead system effect is inevitable – although all leads are placed in fixed locations on the body surface according to the standard, the cardiac axes vary among individuals and for each beat. These result in undesirable signal variations which hamper the visual inspection. Furthermore, note that the impedance inside the

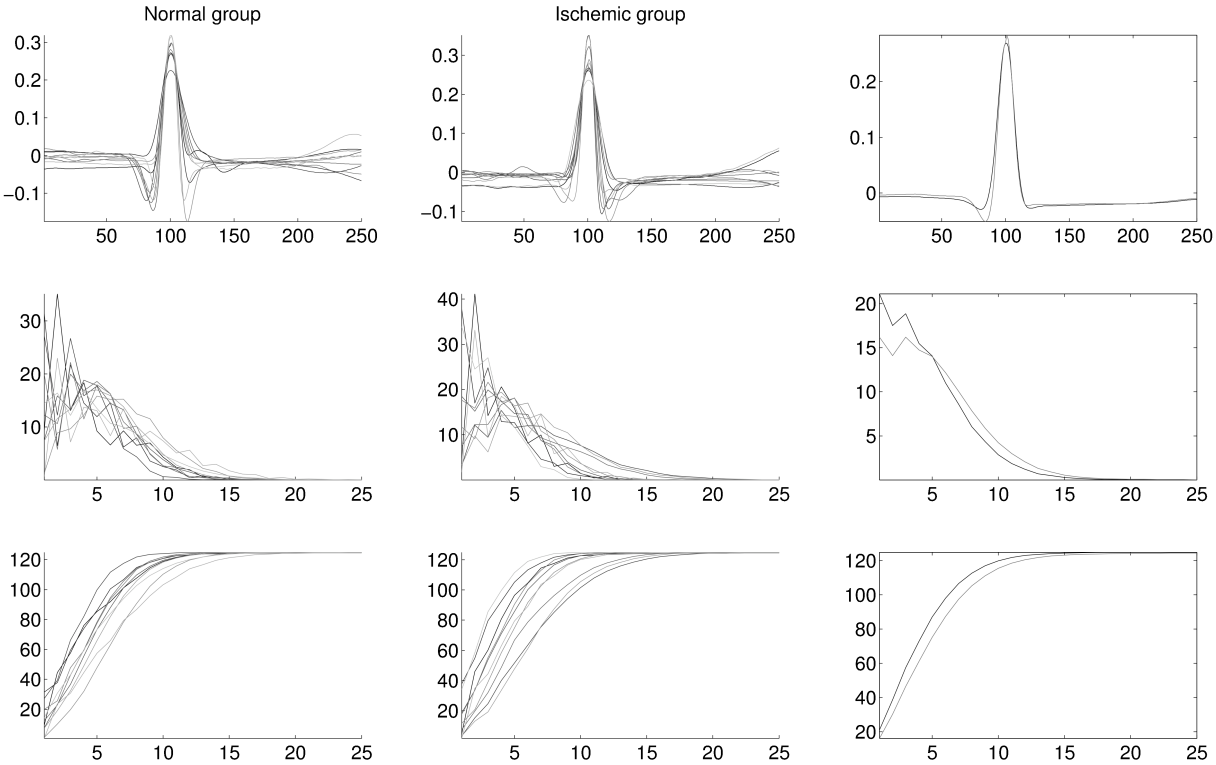

FIGURE 5. Upper left (middle): ten adaptive ECG waveform representations from ten randomly selected subjects in the normal (ischemia) group. We only show the first 250 points for the demonstration purpose. Upper right: the mean adaptive ECG waveform representations of the normal and ischemia groups are respectively plotted in gray and black.Note that a notch on the left-hand side of the peak can be visually observed. Middle left (middle): ten power spectra from ten random subjects in the normal (ischemia) group. We only show the first 25 Fourier modes for the demonstration purpose. Middle right: the mean power spectra of the normal and ischemia groups are respectively plotted in gray and blackNote the obvious shifting of the power spectrum from the high frequency area to the low frequency area in the ischemic group. Lower left (middle): cumulative power spectra from ten random subjects in the normal (ischemia) group. We only show the first 25 cumulative powers for the demonstration purpose. Lower right: the mean cumulative power spectra of the normal and ischemia groups are respectively plotted in gray and black.

chest wall varies proportional to the breathing cycle, that is, the impedance increases as we inhale, and decreases as we exhale. Thus, the respiratory pattern will further compromise the information. The influence of the respiratory pattern is clearly evidenced by the insignificance of the $F_{\max}$-test based on the adaptive lead signal $\mathrm{s}_0^{(i,l)}$ as shown in Table 3.

The significant results of the $F_{\max}$-test based on the power spectrum $P^{(i)}$ and the cumulative power spectrum $f^{(i)}$ confirm our another hypothesis – the power spectrum of the manipulated ECG signal is shifted to the low frequency. Indeed, from the middle right panel in Fig. 5, visually we can see the group shift from the high frequency area to the low frequency area. Due to the group shifting phenomenon, the cumulative power spectrum further enhances the significance of the $F_{\max}$ test, which is shown in Table 3.

In conclusion, with the $F_{\max}$-test, we prove the concept that quantitative analysis of a normalized spectrum from the resting ECG signals contains profound information for screening myocardial ischemia in outpatient settings for those patients with NSR. This finding supports our hypothesis led by the findings in Mor-Avi & Akselrod (1990); Abboud et al. (1987); Pettersson et al. (2000). From the clinical

viewpoint, the most significant advantage of the approach is that it is safer since it does not entail stress-inducing procedures and it is more convenient, affordable, and cost-effective than the existing methods. We emphasize that for more than a hundred years since the introduction of ECG, physicians have been interpreted ECG in the time domain. In their attempts to diagnose myocardial ischemia using extremely advanced and invasive technologies, researchers have almost completely overlooked more adaptive and accessible approaches to recognize myocardial ischemia. A further large scale clinical study is ongoing and the result will be reported in the near future.

TABLE 3. P-values of the GPF and $F_{\max}$ tests for screening stable ischemia. The P-values of the $F_{\max}$-test were obtained based on 10000 bootstrap replicates. Note that the $F_{\max}$-test is not significant if we use the non-normalized adaptive lead signal $\mathbf{s}_0^{(i,l)}$. This indicates the importance of removing the respiratory effect.

	ANOVA	
	$F_{\max}$	GPF
Adaptive lead signal $\mathbf{s}_0^{(i,l)}$	0.0764	0.1317
Adaptive ECG waveform $\mathbf{s}^{(i)}$	0.0006	0.0578
Power spectrum $P^{(i)}$	0.0084	0.1566
Cumulative power spectrum $f^{(i)}$	0.0029	0.1531

6. CONCLUDING REMARKS

In this paper, we proposed and studied the $F_{\max}$-test for the one-way ANOVA problem (2) for functional data under very general conditions. Via intensive simulation studies, we found that the bootstrapped null pdf of the $F_{\max}$-test approximates the associated simulated null pdf rather well; in terms of size controlling, the $F_{\max}$-test outperforms the GPF test of Zhang & Liang (2013); and in terms of power, the $F_{\max}$-test generally has higher powers than the GPF test when the functional data are moderately or highly correlated and the two comparative powers otherwise.

In the preliminary study detailed in Section 5, the $F_{\max}$-test validates the potential of using the adaptive ECG waveform, the power spectrum and the cumulative power spectrum in screening stable ischemia. A further larger scale study is under way so as to confirm the results.

Notice that the $F_{\max}$-test is widely applicable. Actually, it is rather easy to extend the $F_{\max}$-test for various hypothesis testing problems for functional data, because for these hypothesis testing problems it is very easy to construct the associated pointwise F-test (Ramsay & Silverman, 2005; Zhang, 2013). These hypothesis testing problems include two-way ANOVA problems for functional data (Zhang, 2013, ch. 5) and functional linear models with functional responses (Zhang, 2013, ch. 6), among others.

Acknowledgments Zhang's research was supported partially by the National University of Singapore research grant R-155-000-108-112 and by the Mathematics Division, National Center of Theoretical Sciences (Taipei Office). Cheng's research was supported in part by the National Science Council grants NSC97-2118-M-002-001-MY3 and NSC101-2118-M-002-001-MY3, and the Mathematics Division, National Center of Theoretical Sciences (Taipei Office). Chi-Jen Tseng acknowledges Wei-min Brian Chiu for the discussion and data collection. Hau-tieng Wu was supported by the AFOSR grant FA9550-09-1-0643.

REFERENCES

ABBOUD, S., COHEN, R., SELWYN, A. & ET AL (1987). Detection of transient myocardial ischemia by computer analysis of standard and signal-averaged high-frequency electrocardiograms in patients undergoing percutaneous transluminal coronary angioplasty. *Circulation* **76**, 585–96.

BAILEY, J., BERSON, A., GARSON, A. J. & ET AL. (1990). Recommendations for standardization and specifications in automated electrocardiography: bandwidth and digital signal processing. a report for health professionals by an ad hoc writing group of the committee on electrocardiography and cardiac

electrophysiology of the council on clinical cardiology, american heart association. *Circulation* **81**, 730–9.

CLIFFORD, G., AZUAJE, F. & MCSHARRY, P. (2006). *Advanced Methods and Tools for ECG Data Analysis*. Norwood, MA: Artech House.

COX, D. & LEE, J. (2008). Pointwise testing with functional data using the westfall-young randomization method. *Biometrika* **95**, 621–634.

CUEVAS, A., FEBRERO, M. & FRAIMAN, R. (2004). An anova test for functional data. *Comput. Statist. Data Anal.* **4**, 111–122.

DEL RIO, C., MCCONNELL, P., CLYMER, B. & ET AL (2005). Early time course of myocardial electrical impedance during acute coronary artery occlusion in pigs, dogs, and humans. *J. Appl. Physiol.* **99**, 1576–81.

FARAWAY, J. (1997). Regression analysis for a functional response. *Technometrics* **39**, 254–261.

FERRATY, F., ed. (2011). *Recent Advances in Functional Data Analysis and Related Topics*. Springer-Verlag: Berlin Heidelberg.

GIBBONS, R., ABRAMS, J., CHATTERJEE, K. & ET AL (2003). Acc/aha 2002 guideline update for the management of patients with chronic stable angina summary article: a report of the american college of cardiology/american heart association task force on practice guidelines (committee on the management of patients with chronic stable angina). *Circulation* **107**, 149–158.

GIBBONS, R., BALADY, G., BEASLEY, J. & ET AL (2002). Acc/aha 2002 guidelines for exercise testing: executive summary. a report of the american college of cardiology/american heart association task force on practice guidelines (committee to update the 1997 exercise testing guidelines). *Circulation* **106**, 1883–92.

HALL, P., XIA, Y. & XUE, J.-H. (2013). Simple tiered classifiers. *Biometrika* , 431–445.

KLOCKE, F., BAIRD, M., LORELL, B. & ET AL (2003). Acc/aha/asnc guidelines for the clinical use of cardiac radionuclide imaging executive summary: a report of the american college of cardiology/american heart association task force on practice guidelines (acc/aha/asnc committee to revise the 1995 guidelines for the clinical use of cardiac radionuclide imaging). *J. Am. Coll. Cardiol.* **42**, 1318–33.

KORALOV, L. B. & SINAI, Y. G. (2007). *Theory of Probability and Random Processes, Second Edition*. Springer.

LAHA, R. G. & ROHATGI, V. K. (1979). *Probability Theory*. Wiley, New York.

LEVKOV, C. (1987). Orthogonal electrocardiogram derived from the limb and chest electrodes of the conventional 12-lead system. *Med. Biol. Eng. Computing* **25**, 155–64.

MOR-AVI, V. & AKSELROD, S. (1990). Spectral analysis of canine epicardial electrogram. short-term variations in the frequency content induced by myocardial ischemia. *Circ Res* **66**, 1681–91.

NEWEY, W. K. (1991). Uniform convergence in probability and stochastic equicontinuity. *Econometrica* **59**, 1161–1167.

PETTERSSON, J., PAHLM, O., CARRO, E. & ET AL (2000). Changes in high-frequency qrs components are more sensitive than st-segment deviation for detecting acute coronary artery occlusion. *J. Am. Coll. Cardiol.* **36**, 1827–34.

RAMSAY, J. O. & SILVERMAN, B. W. (2005). *Functional Data Analysis*. New York: Springer Series in Statistics. Springer, 2nd ed.

SAMWORTH, R. J. (2012). Optimal weighted nearest neighbor classifiers. *Ann. Statist.* , 2733–2763.

SHEN, Q. & FARAWAY, J. (2004). An f test for linear models with functional responses. *Statist. Sinica* **14**, 1239–1257.

SLAETS, L., CLAESKENS, G. & HUBERT, M. (2012). Phase and amplitude-based clustering for functional data. *Comput. Statist. Data Anal.* , 2360–2374.

SWAN, H. (1979). Mechanical function of the heart and its alteration during myocardial ischemia and infarction. specific reference to coronary atherosclerosis. *Circulation* **60**, 1587–1592.

URHEIM, S., EDVARDSEN, T., TORP, H. & ET AL (2000). Myocardial strain by doppler echocardiography. validation of a new method to quantify regional myocardial function. *Circulation* **102**, 1158–64.

VAN DER VAART, A. W. & WELLNER, J. A. (1996). *Weak Convergence and Empirical Processes*. New York: Springer.

WAND, M. P. & JONES, M. C. (1995). *Kernel Smoothing*. London: Chapman and Hall.

XUE, J.-H. & TITTERINGTON, D. M. (2011). t-tests, f-tests and otsu's methods for image thresholding. *IEEE Trans. Image Processing* , 2392–2396.

ZHANG, J.-T. (2011). Statistical inferences for linear models with functional responses. *Statist. Sinica* **21**, 1431–1451.

ZHANG, J.-T. (2013). *Analysis of Variances for Functional Data*. London: Chapman and Hall.

ZHANG, J.-T. & CHEN, J. W. (2007). Statistical inferences for functional data. *Ann. Statist* **35**, 1052–1079.

ZHANG, J.-T. & LIANG, X. (2013). *One-way ANOVA for functional data via globalizing the pointwise F-test*. Scandinavian Journal of Statistics. To appear.

APPENDIX A.1. APPENDIX: PROOFS OF THE THEORETICAL RESULTS

To give the proofs of the main results, we first state the following lemma whose proof is given in Zhang & Liang (2013).

Lemma A.1. Under Condition A, as $n \to \infty$, we have

$$\mathbf{z}_n(t) \xrightarrow{d} GP_k(\mathbf{0}, \gamma \mathbf{I}_k), \quad \sqrt{n}\left\{\hat{\gamma}(s,t) - \gamma(s,t)\right\} \xrightarrow{d} \mathrm{GP}(0, \varpi), \tag{A.1}$$

where $\varpi\left\{(s_1,t_1),(s_2,t_2)\right\} = \mathrm{E}\left\{v_{11}(s_1)v_{11}(t_1)v_{11}(s_2)v_{11}(t_2)\right\} - \gamma(s_1,t_1)\gamma(s_2,t_2)$. In addition, we have

$$\hat{\gamma}(s,t) = \gamma(s,t) + O_{\mathrm{UP}}\left[n^{-1/2}\right], \tag{A.2}$$

where O_{UP} means "bounded in probability uniformly".

We are now ready to outline the proofs of the main results of this paper.

A.1.1. **Proof of Proposition 2.1.** Under the given conditions and by Lemma A.1, as $n \to \infty$, we have $\mathrm{SSE}_n(t)/(n-k) = \hat{\gamma}(t,t) \xrightarrow{p} \gamma(t,t)$ uniformly for all $t \in \mathcal{T}$, and $\mathbf{z}_n(t) \xrightarrow{d} \mathbf{z}(t) \sim \mathrm{GP}_k(\mathbf{0}, \gamma\mathbf{I}_k)$. Under the null hypothesis, we have $\boldsymbol{\mu}_n(t) \equiv \mathbf{0}$. By Slutsky's theorem, as $n \to \infty$, we have $F_n(t) - R(t) \xrightarrow{p} 0$ for all $t \in \mathcal{T}$ where $R(t) = (k-1)^{-1}\mathbf{z}(t)^T(\mathbf{I}_k - \mathbf{b}\mathbf{b}^T)\mathbf{z}(t)/\gamma(t,t)$ and $\mathbf{I}_k - \mathbf{b}\mathbf{b}^T$ is the limit matrix of $\mathbf{I}_k - \mathbf{b}_n\mathbf{b}_n^T$ as given by (10). Since $\mathcal{T}$ is a finite interval and $F_n(t)$ is continuous over $\mathcal{T}$, it is also equicontinuous. By Theorem 2.1 in Newey (1991), $F_n(t) - R(t) \xrightarrow{p} 0$ uniformly over $\mathcal{T}$. Since we always have $|\sup_{t\in\mathcal{T}} F_n(t) - \sup_{t\in\mathcal{T}} R(t)| \le \sup_{t\in\mathcal{T}} |F_n(t) - R(t)|$, we have $\sup_{t\in\mathcal{T}} F_n(t) - \sup_{t\in\mathcal{T}} R(t) \xrightarrow{p} 0$ which implies that $\sup_{t\in\mathcal{T}} F_n(t) \xrightarrow{d} \sup_{t\in\mathcal{T}} R(t)$. That is $F_{\max} \xrightarrow{d} R_0$ where $R_0 = \sup_{t\in\mathcal{T}} R(t)$.

Notice that $\mathbf{I}_k - \mathbf{b}\mathbf{b}^T$ has the singular value decomposition (11). Let

$$\mathbf{w}(t) = (\mathbf{I}_{k-1}, \mathbf{0})\mathbf{U}^T\mathbf{z}(t)/\sqrt{\gamma(t,t)} = [w_1(t), w_2(t), \cdots, w_{k-1}(t)]^T. \tag{A.3}$$

Then $\mathbf{w}(t) \sim \mathrm{GP}_{k-1}(\mathbf{0}, \gamma_w \mathbf{I}_{k-1})$ where $\gamma_w(s,t) = \gamma(s,t)/\sqrt{\gamma(s,s)\gamma(t,t)}$. It follows that $R(t) = (k-1)^{-1}\mathbf{w}(t)^T\mathbf{w}(t) = (k-1)^{-1}\sum_{i=1}^{k-1} w_i^2(t)$. This completes the proof of Proposition 2.1.

A.1.2. **Proof of Proposition 2.2.** First of all, notice that given the original k samples (1), the bootstrapped k samples $v_{ij}^*(t), j = 1, 2, \cdots, n_i; i = 1, 2, \cdots, k \overset{i.i.d.}{\sim} \mathrm{SP}(0, \hat{\gamma})$ where $\hat{\gamma}(s,t)$ is the pooled sample covariance function (12). That is to say, the bootstrapped k samples satisfy the null hypothesis (2). By Lemma A.1 and under Condition A, as $n \to \infty$, we have $\hat{\gamma}(s,t) \xrightarrow{d} \gamma(s,t)$ uniformly over $\mathcal{T}^2$. Applying Proposition 2.1 leads to the first claim of the proposition and the second claim of the proposition follows immediately. The proposition is then proved.

A.1.3. **Proof of Proposition 2.3.** In the proof of Proposition 2.1, we have showed that under Condition A, as $n \to \infty$, we have $\text{SSE}_n(t)/(n-k) \xrightarrow{p} \gamma(t,t)$ uniformly for all $t \in \mathcal{T}$ and $\mathbf{z}_n(t) \xrightarrow{d} \mathbf{z}(t) \sim \text{GP}_k(\mathbf{0}, \gamma \mathbf{I}_k)$. Similar to the proof of Proposition 2.1, since $\mathcal{T}$ is a finite interval and $F_n(t)$ is equicontinuous over $\mathcal{T}$, by Slutsky's theorem, Theorem 2.1 of Newey (1991), and (19), we can show that as $n \to \infty$, we have $F_{\max} \xrightarrow{d} R_1$ with $R_1 = \sup_{t\in\mathcal{T}} \left\{(k-1)^{-1}[\mathbf{z}(t)+\mathbf{d}(t)]^T(\mathbf{I}_k - \mathbf{b}\mathbf{b}^T)[\mathbf{z}(t)+\mathbf{d}(t)]/\gamma(t,t)\right\}$ where the idempotent matrix $\mathbf{I}_k - \mathbf{b}\mathbf{b}^T$ has the singular value decomposition (11). Let $\mathbf{w}(t)$ be defined as in the proof of Proposition 2.1 and let $\boldsymbol{\delta}(t) = (\mathbf{I}_{k-1}, \mathbf{0})\mathbf{U}^T\mathbf{d}(t)/\sqrt{\gamma(t,t)} = [\delta_1(t), \delta_2(t), \cdots, \delta_{k-1}(t)]^T$. Then $\mathbf{w}(t) \sim \text{GP}_{k-1}(\mathbf{0}, \gamma_w \mathbf{I}_{k-1})$ with $\gamma_w(s,t) = \gamma(s,t)/\sqrt{\gamma(s,s)\gamma(t,t)}$ and $(\mathbf{I}_{k-1}, \mathbf{0}]\mathbf{U}^T[\mathbf{z}(t)+\mathbf{d}(t)] = \mathbf{w}(t) + \boldsymbol{\delta}(t)$. Therefore, $R_1 = \sup_{t\in\mathcal{T}} \left\{(k-1)^{-1}[\mathbf{w}(t)+\boldsymbol{\delta}(t)]^T[\mathbf{w}(t)+\boldsymbol{\delta}(t)]\right\} = \sup_{t\in\mathcal{T}} \left\{(k-1)^{-1}\sum_{i=1}^{k-1}[w_i(t)+\delta_i(t)]^2\right\}$. This completes the proof of Proposition 2.3.

A.1.4. **Proof of Proposition 2.4.** By (21), we first have $P(F_{\max} \geq C_\alpha^*) \geq P(T_n \geq (b-a)C_\alpha^*)$. Notice that under Condition A and by Proposition 2.2, we have $(b-a)C_\alpha^* \xrightarrow{d} (b-a)C_\alpha$ with C_α being the upper 100α percentile of R_0. Under Condition A and the local alternative (18), by the proof of Proposition 3 in Zhang & Liang (2013), we have $P(T_n \geq (b-a)C_\alpha^*) \to 1$ as $\delta \to \infty$. Proposition 2.4 is then proved.

A.1.5. **Proof of Proposition 3.1.** By definition, the random vectors $\mathbf{v}_{ij,M} = (v_{ij}(t_1), \ldots, v_{ij}(t_M))^T$, $j = 1, \ldots, n_i$, $i = 1, 2, \cdots, k$, are i.i.d. with a zero mean vector and an $M \times M$ covariance matrix $\boldsymbol{\Gamma}_M$ whose (p,q) entry is $\text{E}v_{ij}(t_p)v_{ij}(t_q) = \gamma(t_p, t_q)$, $p, q = 1, \ldots, M$. Note that for any finite M, taking $n \to \infty$ is exchangeable with taking maximum over the discretization points $t_1, \ldots, t_M$. Set $\mathbf{z}_{n,M} = [\mathbf{z}_n(t_1)^T, \ldots, \mathbf{z}_n(t_M)^T]^T$ and $\mathbf{z}_M = [\mathbf{z}(t_1)^T, \ldots, \mathbf{z}(t_M)^T]^T$ where $\mathbf{z}_n(t)$ is defined in (9) and $\mathbf{z}(t)$ is defined in the proof of Proposition 2.1. It follows from Lemma A.1 that, under Condition A and as $n \to \infty$, we have

$$\mathbf{z}_{n,M} \xrightarrow{d} \mathbf{z}_M \sim N_{kM}(\mathbf{0}, \boldsymbol{\Gamma}_M \otimes \mathbf{I}_k), \quad \sqrt{n}\left\{vec(\hat{\boldsymbol{\Gamma}}_M) - vec(\boldsymbol{\Gamma}_M)\right\} \xrightarrow{d} N_{M^2}(\mathbf{0}, \mathbf{V}_M), \tag{A.4}$$

where $\otimes$ is the usual Kronecker product of two matrices, $vec(\mathbf{A})$ denotes a column vector obtained via stacking all the column vectors of the matrix $\mathbf{A}$ one by one, and $\mathbf{V}_M$ is an $M^2 \times M^2$ matrix whose $((k_1, l_1), (k_2, l_2))$ entry is $\text{E}\left[v_{11}(t_{k_1})v_{11}(t_{l_1})v_{11}(t_{k_2})v_{11}(t_{l_2})\right] - \gamma(t_{k_1}, t_{l_1})\gamma(t_{k_2}, t_{l_2})$, and $v_{11}(t)$ is the subject-effect function of the first subject of the first group. In addition, we have

$$\hat{\boldsymbol{\Gamma}}_M = \boldsymbol{\Gamma}_M + O_{\text{UP}}\left[n^{-1/2}\right]. \tag{A.5}$$

By (A.4) we have $\text{SSR}_n(t_l)/(k-1) \xrightarrow{d} \mathbf{z}(t_l)^T(\mathbf{I}_k - \mathbf{b}\mathbf{b}^T)\mathbf{z}(t_l)/(k-1)$. Under the given conditions and by (A.4) and (A.5), as $n \to \infty$, we have $\text{SSE}_n(t_l)/(n-k) = \hat{\gamma}(t_l, t_l) \xrightarrow{p} \gamma(t_l, t_l)$ for all $l = 1, \ldots, M$. Under the null hypothesis and by Slusky's Theorem, as $n \to \infty$, we have $F_{\max,M} = \max_{l=1,\ldots,M}\{\text{SSR}_n(t_l)/(k-1)\}\{\text{SSE}_n(t_l)/(n-k)\} \xrightarrow{d} R_{0,M}$ where $R_{0,M}$ is defined by

$$R_{0,M} = \max_{l=1,\ldots,M}\left[\left\{(k-1)\gamma(t_l, t_l)\right\}^{-1}\mathbf{z}(t_l)^T(\mathbf{I}_k - \mathbf{b}\mathbf{b}^T)\mathbf{z}(t_l)\right],$$

and $\mathbf{I}_k - \mathbf{b}\mathbf{b}^T$ is the limit matrix of $\mathbf{I}_k - \mathbf{b}_n\mathbf{b}_n^T$; see (10). Note that under the null hypothesis, we have $\boldsymbol{\mu}(t_l)^T(\mathbf{I}_k - \mathbf{b}\mathbf{b}^T)\boldsymbol{\mu}(t_l) \equiv \mathbf{0}, l = 1, \ldots, M$. For $l = 1, \ldots, M$, set

$$\mathbf{w}_M(l) = (\mathbf{I}_{k-1}, \mathbf{0})\mathbf{U}^T\mathbf{z}_M(l)/\sqrt{\gamma(t_l, t_l)} = [w_{1,M}(l), w_{2,M}(l), \cdots, w_{k-1,M}(l)]^T, \tag{A.6}$$

where $\mathbf{U}$ comes from the singular value decomposition (11) of $\mathbf{I}_k - \mathbf{b}\mathbf{b}^T$. Then we have $R_{0,M} = \max_{l=1,\ldots,M}\left\{(k-1)^{-1}\mathbf{w}_M(l)^T\mathbf{w}_M(l)\right\} = \max_{l=1,\ldots,M}\left\{(k-1)^{-1}\sum_{i=1}^{k-1} w_{i,M}^2(l)\right\}$. Let $\mathbf{w}_{i,M} = (w_i(t_1), \ldots, w_i(t_M))^T, i = 1, \cdots, k-1$. Then $\mathbf{w}_{1,M}, \ldots, \mathbf{w}_{k-1,M} \overset{i.i.d.}{\sim} N_M(\mathbf{0}, \boldsymbol{\Gamma}_{w,M})$ where the (p,q) entry of $\boldsymbol{\Gamma}_{w,M}$ is $\gamma_w(t_p, t_q), p, q = 1, \ldots, M$. This completes the proof of $F_{\max,M} \xrightarrow{d} R_{0,M}$ as $n \to \infty$.

Next, by Condition A5 on $\gamma(s,t)$ and a direct calculation by the definition of Hölder's continuity, the covariance function $\gamma_w(s,t)$ of the Gaussian process $\omega_i(t)$ defined in (A.3) is in $C^\beta(\mathcal{T} \times \mathcal{T})$. Thus,

Kolmogorov's Theorem (Koralov & Sinai, 2007, Theorem 18.19) says that, for all $i = 1, \ldots, k-1$, there exists a continuous modification $W_i(t), t \in \mathcal{T}$ of $\omega_i(t), t \in \mathcal{T}$ and an event subspace $\Omega(M)$ with $P(\Omega(M)) \to 1$ as $M \to \infty$, so that for all events in $\Omega(M)$, $W_i(t)$ is Hölder continuous with exponent $0 < \tilde{\beta} < \beta$ and Hölder's modulus $c_{\tilde{\beta}} = 2/(1-2^{-\tilde{\beta}})$. Thus, from now on we work with $\{W_i(t)\}_{i=1}^{k-1}$ instead of $\{\omega_i(t)\}_{i=1}^{k-1}$ and use the same notation for the versions of R_0 and $R_{0,M}$ based on the continuous modifications:

$$R_0 \stackrel{d}{=} \sup_{t\in\mathcal{T}} \Big\{(k-1)^{-1}\sum_{i=1}^{k-1} W_i^2(t)\Big\}, \quad R_{0,M} \stackrel{d}{=} \max_{l=1,\ldots,M} \Big\{(k-1)^{-1}\sum_{i=1}^{k-1} W_{i,M}^2(l)\Big\},$$

where $W_{i,M}(l) = W_i(t_l), l = 1, \ldots, M; i = 1, \ldots, k-1$. Clearly $(k-1)^{-1}\sum_{i=1}^{k-1} W_i^2(t)$ is also Hölder continuous with exponent $\tilde{\beta}$ and Hölder's modulus $\tilde{c} = c_{\tilde{\beta}}^2$. Since $\mathcal{T}$ is compact, the supremum of $\sum_{i=1}^{k-1} W_i^2(t)$ is achieved at some $t' \in [t_{l'-1}, t_{l'+1}]$. By Hölder's continuity of the process, we have

$$\Big|(k-1)^{-1}\sum_{i=1}^{k-1} W_{i,M}^2(l') - \sup_{t\in[t_{l'-1},t_{l'+1}]} (k-1)^{-1}\sum_{i=1}^{k-1} W_i^2(t)\Big| \le \tilde{c}\tau_M^{\tilde{\beta}}.$$

Suppose the maximum of $\sum_{i=1}^{k-1} W_{i,M}^2(l)$ is achieved at l'' instead of l', we must have

$$(k-1)^{-1}\sum_{i=1}^{k-1} W_{i,M}^2(l') \le (k-1)^{-1}\sum_{i=1}^{k-1} W_{i,M}^2(l'') \le (k-1)^{-1}\sum_{i=1}^{k-1} W_i^2(t'),$$

where the last inequality holds by definition. Thus, for all events in $\Omega(M)$, we have

$$\big|R_0 - R_{0,M}\big| \le \tilde{c}\tau_M^{\tilde{\beta}}. \tag{A.7}$$

A.1.6. **Proof of Proposition 3.2.** Note that the k bootstrapped samples $\{\mathbf{v}_{ij,M}^*\}_{j=1}^{n_i}, i = 1, \cdots, k$ are i.i.d. with mean vector $\mathbf{0}$ and covariance matrix $\hat{\mathbf{\Gamma}}_M$ whose (p,q) entry is $\hat{\gamma}(t_p, t_q), p, q = 1, \ldots, M$. That is to say, the bootstrapped k samples satisfy the discretized null hypothesis (23). By (A.4) and (A.5), and under Condition A, as $n \to \infty$, we have $\hat{\mathbf{\Gamma}}_M \stackrel{d}{\to} \mathbf{\Gamma}_M$ uniformly. Applying the same arguments as in the proof of $F_{\max,M} \stackrel{d}{\to} R_{0,M}$ to the k bootstrapped samples $\{\mathbf{v}_{ij,M}^*\}_{j=1}^{n_i}, i = 1, \cdots, k$, leads to the claim that $F_{\max,M}^* \stackrel{d}{\to} R_{0,M}$ as $n \to \infty$.

A.1.7. **Proof of Proposition 3.3.** As in the proof of Proposition 3.1, under Condition A, $\mathrm{SSE}_n(t_l)/(n-k) \stackrel{p}{\to} \gamma(t_l, t_l)$ and $\mathbf{z}_{n,M} \stackrel{d}{\to} \mathbf{z}_M \sim N_{kM}(\mathbf{0}, \mathbf{\Gamma}_M \otimes \mathbf{I}_k)$ as $n \to \infty$. Under H_1, we have $\mu_i(t_l) = \mu_0(t_l) + n_i^{-1/2} d_i(t_l), l = 1, \ldots, M;\ i = 1, 2, \cdots, k$. It follows that $\boldsymbol{\mu}(t_l) = \mu_0(t_l)\mathbf{1}_k + \mathrm{diag}(n_1^{-1/2}, \ldots, n_k^{-1/2})\mathbf{d}(t_l)$, $l = 1, \ldots, M$ where $\boldsymbol{\mu}(t) = [\mu_1(t), \ldots, \mu_k(t)]^T$ and $\mathbf{d}(t) = [d_1(t), \ldots, d_k(t)]^T$ as defined before. Then we have $\boldsymbol{\mu}_n(t_l) = \mathrm{diag}(n_1^{1/2}, \ldots, n_k^{1/2})\boldsymbol{\mu}(t_l) = \mu_0(t_l)\mathbf{b}_n + \mathbf{d}(t_l)$. Since $(\mathbf{I}_k - \mathbf{b}_n\mathbf{b}_n^T/n)\mathbf{b}_n = \mathbf{0}$, under H_1, we have $\mathrm{SSR}_n(t_l) = \big[\mathbf{z}_n(t_l) + \mathbf{d}(t_l)\big]^T(\mathbf{I}_k - \mathbf{b}_n\mathbf{b}_n^T/n)\big[\mathbf{z}_n(t_l) + \mathbf{d}(t_l)\big]$. Hence, as $n \to \infty$, we have $F_{\max,M} \stackrel{d}{\to} R_{1,M}$. Let $\mathbf{w}_M(l)$ be as defined in (A.6) and let $\boldsymbol{\delta}_M(l) = \boldsymbol{\delta}(t_l) = (\mathbf{I}_{k-1}, \mathbf{0})\mathbf{U}^T\mathbf{d}(t_l)/\sqrt{\gamma(t_l, t_l)} = [\delta_{1,M}, \delta_{2,M}, \cdots, \delta_{k-1,M}]^T$ where $\delta_{i,M}(l) = \delta_i(t_l), l = 1, \ldots, M$. Thus, $(\mathbf{I}_{k-1}, \mathbf{0}]\mathbf{U}^T[\mathbf{z}(t_l) + \mathbf{d}(t_l)]/\sqrt{\gamma(t_l, t_l)} = \mathbf{w}_M(l) + \boldsymbol{\delta}_M(l)$. Therefore, we have

$$\begin{aligned} R_{1,M} &= \max_{l=1,\ldots,M} \Big\{(k-1)^{-1}[\mathbf{w}_M(l) + \boldsymbol{\delta}_M(l)]^T[\mathbf{w}_M(l) + \boldsymbol{\delta}_M(l)]\Big\} \\ &= \max_{l=1,\ldots,M} \Big\{(k-1)^{-1}\sum_{i=1}^{k-1}[w_{i,M}(l) + \delta_{i,M}(l)]^2\Big\}. \end{aligned}$$

Next, using the same arguments in the proof of (A.7), we can show that there exists an event space $\Omega(M)$ with $P(\Omega(M)) \to 1$ such that conditional on $\Omega(M)$, for all $i = 1, \ldots, k-1$, we have a continuous modification $W_i(t)$ of $\omega_i(t)$ defined in (A.3) so that $W_i(t)$ is Hölder continuous with exponent $0 < \tilde{\beta} <$

$\beta/2$ and Hölder's modulus $c_{\tilde{\beta}} = 2/(1-2^{-\tilde{\beta}})$. We use the same notation for the versions of R_1 and $R_{1,M}$ based on the continuous modifications:

$$R_1 \stackrel{d}{=} \sup_{t\in\mathcal{T}} \Big\{(k-1)^{-1}\sum_{i=1}^{k-1}[W_i(t)+\delta_i(t)]^2\Big\},\ R_{1,M} \stackrel{d}{=} \max_{l=1,\ldots,M} \Big\{(k-1)^{-1}\sum_{i=1}^{k-1}[W_{i,M}(l)+\delta_{i,M}(l)]^2\Big\},$$

where $W_{i,M}(l) = W_i(t_l), l = 1,\ldots,M$. Clearly, under the assumption on $d_i(t)$, we know $(k-1)^{-1}\sum_{i=1}^{k-1}[W_i(t)+\delta_i(t)]^2$ is also Hölder continuous with exponent $\tilde{\beta}$ and Hölder's modulus $\tilde{c} = 2(c_{\tilde{\beta}}^2 + c_\delta^2)$, where c_δ is the maximum of the Hölder's modulus of $d_i(t)$, $i = 1,\ldots,k$. Again, by the same arguments as those leading to (A.7), for all events in $\Omega(M)$ we have $\big|R_1 - R_{1,M}\big| \le \tilde{c}\tau_M^{\tilde{\beta}}$.

DEPARTMENT OF STATISTICS AND APPLIED PROBABILITY, NATIONAL UNIVERSITY OF SINGAPORE, SINGAPORE
E-mail address: stazjt@nus.edu.sg

DEPARTMENT OF MATHEMATICS, NATIONAL TAIWAN UNIVERSITY, TAIWAN
E-mail address: cheng@math.ntu.edu.tw

CARDIOVASCULAR RESEARCH INSTITUTE, FOOYIN UNIVERSITY HOSPITAL, TAIWAN
E-mail address: chijen.tseng@gmail.com

DEPARTMENT OF MATHEMATICS, STANFORD UNIVERSITY, USA
E-mail address: hauwu@stanford.edu